Supporting Information

Architecture-supramolecularly engineered cascade regulates NIR-II J-aggregates to improve photodynamic therapy

Huizhe Wang[1], Huijia Liu[1], Wenqing Li[1], Jiaqi Zhang[1], Shuai Li[1], Jingzhe Zang[1], Li Liu[1], Peng Wang[1*]

[1]*Department of Biomedical Engineering, School of Engineering, China Pharmaceutical University, Nanjing 210009, China*

Corresponding email: wangpeng@cpu.edu.cn

Table of Contents

Synthesis Rote

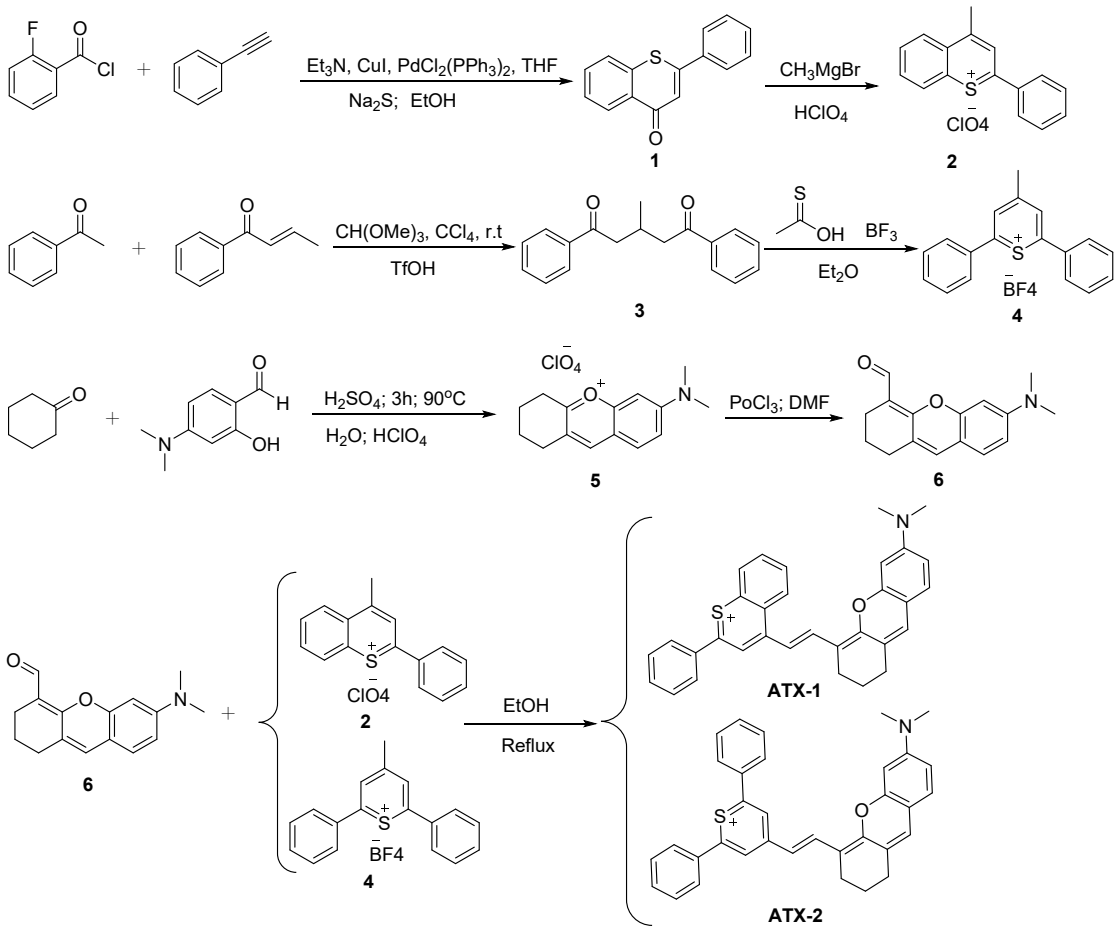

Scheme S1. Synthetic route of **ATX-1** and **ATX-2**.

*Synthesis of **1***

$PdCl_2(PPh_3)_2$ (15 mg, 0.02 mmol), CuI (8 mg, 0.04 mmol), and THF (4 ml) were added to a 10 ml microwave tube under a nitrogen atmosphere. Then, 2-fluorobenzoyl chloride (150 μL, 1.25 mmol), phenylacetylene (120 μL, 1.00 mmol), and Et_3N (140 μL, 1.05 mmol) were added to the above mixture. The reaction mixture was stirred at r.t. for 1 h. Finally, $Na_2S{\cdot}9H_2O$ (144 mg, 1.50 mmol) followed by EtOH (1 mL) were added to this suspension, and the reaction mixture was heated at 90 °C in the microwave cavity for 90 min. After cooling to r.t., the solvent was removed under reduced pressure, and the crude product was purified by silica gel column chromatography (PE-EtOAc) to obtain product **1** as a yellow solid. Yield: 70%. ^{1}H NMR (300 MHz, $CDCl_3$) δ 8.57 - 8.50 (m, 1H), 7.69 (d, J = 2.1 Hz, 1H), 7.68 - 7.66 (m, 1H), 7.65 - 7.62 (m, 1H), 7.60 (dd, J = 8.0, 1.6 Hz, 1H), 7.55 (dd, J = 8.0, 1.8 Hz,

1H), 7.50 (d, *J* = 2.0 Hz, 2H), 7.49 (d, *J* = 1.9 Hz, 1H), 7.24 (s, 1H). ^{13}C NMR (101 MHz, $CDCl_3$) δ 180.92, 153.11, 137.75, 136.61, 131.68, 130.96, 130.90, 129.36, 128.65, 127.84, 127.03, 126.57, 123.48.

*Synthesis of **2***

1.0 M CH_3MgBr (5.34 mL) was added dropwise to a solution of compound **1** (477 mg, 2.00 mmol) in anhydrous THF (10 mL). After stirring at room temperature for 2 h under nitrogen, the solution was poured into 10% aqueous $HClO_4$ (20 mL) and allowed to stir for 5 min before the solid was isolated by filtration. The resulting solid was dried to give **2** as an orange-red solid. Yield: 78%. ^{1}H NMR (300 MHz, CD_3CN) δ 8.88 (s, 1H), 8.86 - 8.79 (m, 1H), 8.66 - 8.60 (m, 1H), 8.30 - 8.19 (m, 2H), 8.17 - 8.11 (m, 2H), 7.89 - 7.82 (m, 1H), 7.80 - 7.72 (m, 2H), 3.28 (s, 3H). ^{13}C NMR (101 MHz, CD_3CN) δ 176.15, 168.25, 143.09, 135.96, 135.86, 135.21, 134.15, 132.28, 132.05, 131.50, 131.27, 129.96, 129.58, 24.54.

*Synthesis of **3***

To a solution of acetophenone (280 μL, 2.40 mmol) in carbon tetrachloride (4 mL), trimethyl orthoformate (53 μL, 0.48 mmol) was added under ice bath conditions. After stirring for 5 min, trifluoroacetic acid (42 μL, 0.48 mmol) was added to the above mixture, and phenylacryl ketone (56 μL, 0.48 mmol) was added dropwise after stirring for another 2 h at this temperature. After which, the mixture was stirred at room temperature for 6 - 8 h and then the solvent was removed under vacuum followed by silica gel column chromatography (PE-EtOAc) to obtain the yellow oily product **3** in 48% yield. ^{1}H NMR (400 MHz, $CDCl_3$) δ 8.00 (d, *J* = 7.3 Hz, 4H), 7.56 (t, *J* = 7.3 Hz, 2H), 7.46 (t, *J* = 7.6 Hz, 4H), 3.23 - 3.13 (m, 2H), 2.89 (d, *J* = 6.0 Hz, 1H), 2.86 (m, 2H), 1.08 (d, *J* = 6.1 Hz, 3H). ^{13}C NMR (101 MHz, $CDCl_3$) δ 199.72, 137.11, 133.15, 128.70, 128.27, 45.47, 26.69, 20.37.

*Synthesis of **4***

Compound 3 (4.00 mmol), thioacetic acid (8.40 mmol), and boron trifluoride ether complex (25 mmol)were added in ether (3.50 ml)， and the mixture was refluxed for 1.5 h under dry air. Finally, a small amount of water and a large amount

of ether were added to the above mixture, which was filtered and dried to give the yellow powder thiopyronium salt **4**. Yield: 78%. ^{1}H NMR (400 MHz, CD_3CN) δ 8.73 (s, 2H), 8.04 - 7.99 (m, 4H), 7.82 - 7.76 (m, 2H), 7.75 - 7.71 (m, 4H), 2.95 (s, 3H). ^{13}C NMR (101 MHz, CD_3CN) δ 169.86, 168.15, 135.04, 134.83, 134.68, 131.39, 129.51, 26.31.

*Synthesis of **5***

Cyclohexanone (413 μL, 4.00 mmol) was added into 4.38 ml of concentrated sulfuric acid under the condition of the ice bath and stirred for 20 min. Then, 4-(dimethylamino) salicylaldehyde was added and stirred at 90 ℃ for 3 h. After cooling, it was poured slowly into the crushed ice, 440 μL of perchloric acid was added, stirred thoroughly, and left to stand at 4 ℃ for 24 h. A solid was precipitated, and the product was obtained by filtration in red-brown color. Yield: 92%. ^{1}H NMR (300 MHz, $CDCl_3$) δ 8.45 (s, 1H), 7.91 (d, J = 9.5 Hz, 1H), 7.31 (dd, J = 9.5, 2.4 Hz, 1H), 6.84 (d, J = 2.0 Hz, 1H), 3.35 (s, 6H), 3.04 (t, J = 5.9 Hz, 2H), 2.86 (t, J = 6.1 Hz, 2H), 2.00 (td, J = 6.1, 2.6 Hz, 2H), 1.92 - 1.83 (m, 2H). ^{13}C NMR (101 MHz, $CDCl_3$) δ 171.29, 159.85, 158.19, 151.11, 132.76, 122.77, 119.68, 118.95, 95.70, 77.16, 41.44, 29.34, 26.40, 21.49, 21.30.

*Synthesis of **6***

Compound 5 (761 mg, 3.35 mmol) was dissolved in 5 ml of DMF, and trichlorophosphorus (615 μL, 6.7 mmol) was added dropwise at 0 °C, the reaction was monitored at room temperature and then poured into crushed ice to burst, the aqueous phase was extracted by CH_2Cl_2, the organic phase was collected and concentrated, a small amount of methanol was solubilized, and was added dropwise to NaOH solution, hydrochloric acid was added and adjusted to neutral, the reaction was extracted by CH_2Cl_2 and the organic phase was collected and concentrated. The crude product was purified by silica gel column chromatography (PE-EtOAC) to obtain a yellow solid with a 78% yield. ^{1}H NMR (300 MHz, $CDCl_3$) δ 10.27 (s, 1H), 7.01 (d, J = 8.5 Hz, 1H), 6.63 (s, 1H), 6.44 (dd, J = 8.5, 2.5 Hz, 1H), 6.39 (d, J = 2.3 Hz, 1H), 3.01 (s, 6H), 2.57 - 2.51 (m, 2H), 2.43 (t, J = 6.1 Hz, 2H), 1.73 - 1.64 (m, 2H). ^{13}C NMR (101 MHz,

$CDCl_3$) δ 187.28, 162.03, 153.89, 152.04, 128.20, 127.47, 123.80, 111.60, 110.95, 108.27, 97.96, 40.40, 29.95, 21.70, 20.70.

*General Procedure for synthesis of **ATX-1**, **ATX-2***

Compound **6** (255 mg, 1 mmol), and compound **2** (404 mg, 1.2 mmol) or **4** (420 mg, 1.2 mmol) were dissolved in EtOH (10 mL) under a nitrogen atmosphere, the mixture was refluxed overnight and then the solvent was removed under reduced pressure to give the crude product, which was purified by silica gel flash chromatography to afford compounds **ATX-1**, and **ATX-2** as dark green solid.

ATX-1 yield: 46%. ^{1}H NMR (400 MHz, DMSO-d_6) δ 8.51 (d, J = 13.0 Hz, 1H), 8.39 (d, J = 6.1 Hz, 1H), 8.34 (s, 1H), 8.07 (s, 1H), 7.91 (dd, J = 6.5, 2.9 Hz, 2H), 7.81 (d, J = 9.2 Hz, 1H), 7.72 - 7.67 (m, 1H), 7.59 - 7.54 (m, 4H), 7.37 - 7.30 (m, 2H), 7.27 (d, J = 9.7 Hz, 2H), 3.29 (s, 6H), 2.97 - 2.90 (m, 2H), 2.85 (t, J = 5.8 Hz, 2H), 1.93 - 1.86 (m, 2H). ^{13}C NMR (126 MHz, DMSO-d_6) δ 162.82, 157.30, 156.28, 145.72, 136.24, 133.59, 132.65, 130.85, 130.37, 130.05, 129.26, 128.74, 128.67, 127.33, 126.49, 125.09, 124.04, 117.17, 116.72, 96.06, 40.38, 27.36, 24.79, 20.49. HRMS (ESI): calcd. for $C_{33}H_{28}NOS^+$ $[M+H]^+$ 474.1886, found 474.1873.

ATX-2 yield: 38%. ^{1}H NMR (400 MHz, CD_3CN) δ 8.39 (d, J = 13.8 Hz, 1H), 7.91 (d, J = 13.0 Hz, 1H), 7.79 - 7.75 (m, 2H), 7.74 (s, 1H), 7.70 (s, 1H), 7.61 - 7.57 (m, 2H), 7.54 (d, J = 7.1 Hz, 5H), 7.50 (d, J = 9.1 Hz, 2H), 7.00 (dd, J = 9.1, 2.5 Hz, 1H), 6.91 (d, J = 2.4 Hz, 1H), 6.52 (d, J = 13.7 Hz, 1H), 3.16 (s, 6H), 2.76 - 2.71 (m, 2H), 2.69 (t, J = 5.9 Hz, 2H), 1.28 (d, J = 7.0 Hz, 2H). ^{13}C NMR (101 MHz, CD_3CN) δ 164.57, 158.07, 156.61, 148.00, 143.52, 136.73, 131.84, 131.02, 130.58, 130.44, 125.43, 122.36, 121.74, 116.70, 115.78, 97.13, 40.94, 28.96, 25.81, 21.56. HRMS (ESI): calcd. for $C_{34}H_{30}NOS^+$ $[M+H]^+$ 500.2043, found 500.2035.

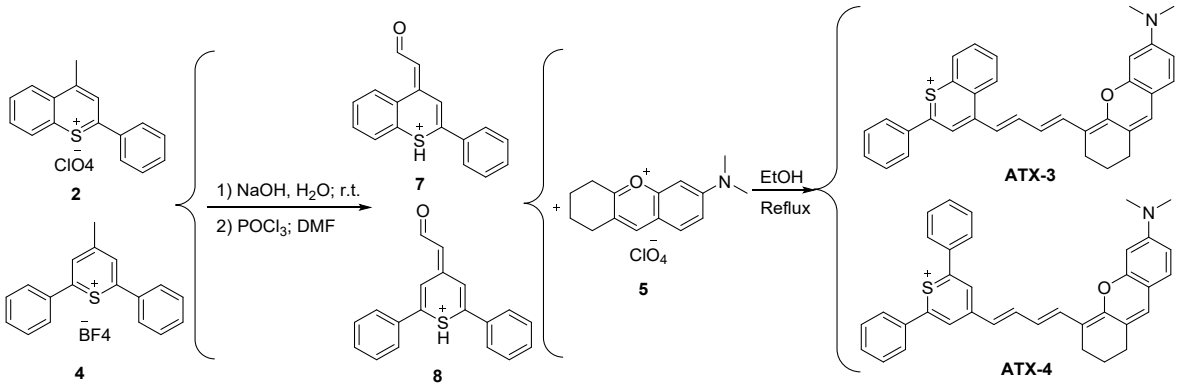

Scheme S2. Synthetic route of **ATX-3** and **ATX-4**.

General Procedure for Synthesis of 7 and 8

Compounds **7** and **8** were synthesized according to previous literature.[1] Briefly, compound **2** (1.01 g, 3.00 mmol) or **4** (1.05 g, 3.00 mmol) was added into a solution of potassium hydroxide (1.0 M, 10 mL). The suspension was stirred for 15 min at room temperature. The resulting oil was extracted with Et_2O and washed with saturated NaCl (aqueous) repeatedly followed by drying over anhydrous sodium sulfate. Evaporation of the solvent gave the oily product and it was used directly in the next step without purification.

$POCl_3$ (300 μL) was added dropwise to cold and dry DMF (2 mL) under a nitrogen atmosphere, and the temperature was kept below 10 ℃. After adding a mixture of DMF (2 mL) with the above oily product (1.00 mmol) in the reaction vessel, the reaction solution was heated at 35℃ for 45 min. Then the reaction solution was poured into ice water and the mixture was basified to pH 10.0 by the addition of saturated sodium hydroxide solution. The product was filtered off to afford **7** or **8** as yellow solids.

Compound **7**: yield: 45%. ^{1}H NMR (400 MHz, $CDCl_3$) δ 10.26 (d, J = 6.6 Hz, 1H), 8.30 (s, 1H), 7.99 (d, J = 7.7 Hz, 1H), 7.68 (dd, J = 5.9, 2.2 Hz, 2H), 7.50 - 7.45 (m, 5H), 7.43 (d, J = 7.7 Hz, 1H), 6.47 (d, J = 6.6 Hz, 1H). ^{13}C NMR (101 MHz, $CDCl_3$) δ 189.36, 146.51, 142.97, 137.38, 134.19, 130.28, 130.12, 129.27, 128.16, 127.34, 126.88, 126.01, 117.21, 115.51.

Compound **8**: yield 47%. ^{1}H NMR (400 MHz, $CDCl_3$) δ 9.97 (d, J = 6.2 Hz, 1H), 8.29 (s, 1H), 7.68 - 7.63 (m, 2H), 7.62 - 7.57 (m, 2H), 7.49 - 7.45 (m, 6H), 6.93 (s, 1H), 5.74 (d, J = 6.2 Hz, 1H). ^{13}C NMR (101 MHz, $CDCl_3$) δ 188.39, 147.82, 145.99, 145.22, 137.10, 136.88, 130.37, 130.31, 129.32, 126.84, 126.57, 124.50, 119.66, 117.17.

*General Procedure for synthesis of **ATX-3**, **ATX-4***

Compound **7** (265 mg, 1.00 mmol) or compound **8** (291 mg, 1.00 mmol), and compound **5** (394 mg, 1.20 mmol) were dissolved in EtOH (10 mL) under nitrogen atmosphere, the mixture was refluxed overnight and then the solvent was removed under reduced pressure to give the crude product, which was purified by silica gel flash chromatography to afford compounds **ATX-3**, and **ATX-4** as a dark brown powder

ATX-3 yield: 31%. ^{1}H NMR (400 MHz, DMSO-d_6) δ 8.44 (d, J = 12.9 Hz, 1H), 8.35 (s, 1H), 8.27 (s, 1H), 8.02 (s, 1H), 7.92 - 7.85 (m, 2H), 7.78 (s, 1H), 7.64 (s, 2H), 7.54 (dd, J = 7.1, 4.0 Hz, 5H), 7.32 - 7.21 (m, 3H), 7.16 (s, 1H), 3.26 (s, 6H), 2.92 - 2.86 (m, 2H), 2.83 - 2.75 (m, 2H), 1.91 - 1.82 (m, 2H). ^{13}C NMR (126 MHz, DMSO-d_6) δ 162.84, 157.31, 156.28, 145.74, 136.27, 130.85, 130.35, 130.04, 129.25, 128.76, 128.67, 127.33, 126.51, 124.05, 117.17, 116.73, 96.08, 40.38, 27.37, 24.79, 20.48. HRMS (ESI): calcd. for $C_{34}H_{30}NOS^+$ $[M+H]^+$ 500.2043, found 500.2035.

ATX-4 yield: 28%. ^{1}H NMR (400 MHz, DMSO-d_6) δ 8.46 (s, 1H), 8.05 (d, J = 4.2 Hz, 2H), 7.84 (d, J = 37.5 Hz, 7H), 7.58 (s, 7H), 7.19 - 7.09 (m, 2H), 6.74 (d, J = 13.5 Hz, 1H), 3.20 (s, 6H), 2.77 (s, 2H), 2.72 (d, J = 6.3 Hz, 2H), 1.89 - 1.80 (m, 2H). ^{13}C NMR (126 MHz, DMSO-d_6) δ 153.96, 151.85, 145.00, 138.14, 136.70, 136.02, 134.28, 133.00, 131.54, 130.81, 129.23, 129.20, 129.09, 128.94, 128.16, 127.97, 125.62, 119.58, 118.06, 116.15, 111.29, 41.31, 28.34, 27.29, 23.28. HRMS (ESI): calcd. for $C_{36}H_{32}NOS^+$ $[M+H]^+$ 526.2299, found 526.2208.

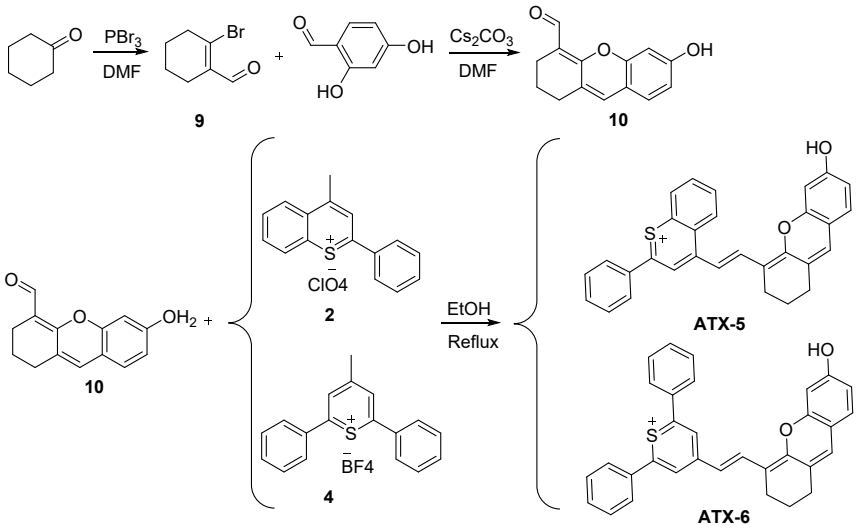

Scheme S3. Synthetic route of **ATX-5** and **ATX-6**.

*Synthesis of **9***

PBr_3 (900 μL, 9.50 mmol) was slowly added to the solution of DMF (1.2 mL, 15.50 mmol) and $CHCl_3$ (10 mL) at 0 °C. After the mixture was stirred for 1 h, cyclohexanone (400 μL, 3.90 mmol) dissolved in $CHCl_3$ (10 mL) was added and the mixture was continued stirring at 25 °C overnight. The mixture was poured into ice and solid $NaHCO_3$ was slowly added until pH = 7. The layers were separated and the aqueous layer was extracted with CH_2Cl_2 (100 mL). The organic layer was dried over Na_2SO_4, and the solvent was removed by evaporation under reduced pressure to provide compound **9** as a yellow oil. Yield: 80%. ^{1}H NMR (300 MHz, $CDCl_3$) δ 9.87 (s, 1H), 2.62 (s, 2H), 2.14 (s, 2H), 1.64 (s, 2H), 1.57 (s, 2H). ^{13}C NMR (101 MHz, $CDCl_3$) δ 193.80, 143.74, 135.33, 38.89, 25.05, 24.32, 21.14.

*Synthesis of **10***

Compound **9** (756 mg, 4.00 mmol), 2,4-Dihydroxybenzaldehyde (276 mg, 2.00 mmol), and ATX_2CO_3 (1.95 g, 6.00 mmol) were dissolved in anhydrous DMF (20 mL). The mixture was stirred for 24 h at 25 °C. The insoluble substance was then filtered on a pad of silica gel and the filtrate was concentrated. The resulting residue was dissolved in CH_2Cl_2 (100 mL), followed by washing with water three times and drying with Na_2SO_4. The solvent was removed by evaporation under reduced pressure, and the residue was subjected to silica gel chromatography with CH_2Cl_2/EtOAc as

eluent to afford compound **10** as a deep yellow solid. Yield: 64%. ^{1}H NMR (400 MHz, DMSO-d_6) δ 10.20 (d, J = 5.7 Hz, 1H), 7.19 (d, J = 8.2 Hz, 1H), 6.93 (s, 0H), 6.66 – 6.56 (m, 1H), 2.28 (t, J = 5.5 Hz, 2H), 1.62 - 1.57 (m, 3H), 1.24 (d, J = 10.6 Hz, 2H). ^{13}C NMR (101 MHz, DMSO-d_6) δ 186.14, 160.35, 159.73, 152.76, 128.16, 127.66, 124.73, 113.05, 112.03, 111.31, 101.88, 28.96, 21.24, 20.02.

*General Procedure for synthesis of **ATX-5**, **ATX-6***

Compound **10** (228 mg, 1 mmol), and compound **2** (404 mg, 1.2 mmol) or **4** (420 mg, 1.2 mmol) were dissolved in EtOH (10 mL) under a nitrogen atmosphere, the mixture was refluxed overnight and then the solvent was removed under reduced pressure to give the crude product, which was purified by silica gel flash chromatography to afford compounds **ATX-5**, and **ATX-6** as dark green solid.

ATX-5: yield: 36%. ^{1}H NMR (400 MHz, DMSO-d_6) δ 8.21 (s, 1H), 8.03 (d, J = 6.7 Hz, 1H), 7.82 (d, J = 6.5 Hz, 3H), 7.55 (dt, J = 13.2, 7.0 Hz, 4H), 7.47 (s, 3H), 7.16 (s, 2H), 6.63 (s, 1H), 6.51 (d, J = 24.0 Hz, 1H), 2.87 (d, J = 14.8 Hz, 2H), 2.72 (d, J = 8.2 Hz, 2H), 1.84 (s, 2H). ^{13}C NMR (126 MHz, DMSO-d_6) δ 158.22, 155.70, 146.83, 143.68, 137.57, 136.93, 131.76, 130.62, 130.24, 129.91, 128.54, 127.48, 126.70, 125.94, 125.58, 125.31, 123.46, 121.02, 120.98, 114.39, 113.59, 113.54, 100.81, 29.44, 28.01, 23.95. HRMS (ESI): calcd. for $C_{30}H_{23}O_2S^+$ $[M+H]^+$ 447.1413, found 447.1407.

ATX-6: yield: 41%. ^{1}H NMR (500 MHz, DMSO-d_6) δ 8.85 (s, 1H), 8.68 (s, 1H), 8.04 (s, 4H), 7.71 (d, J = 5.9 Hz, 7H), 7.61 - 7.55 (m, 1H), 7.48 (s, 2H), 7.19 - 7.05 (m, 2H), 2.70 (d, J = 27.5 Hz, 4H), 1.86 (p, J = 6.6, 4.9 Hz, 2H). ^{13}C NMR (101 MHz, DMSO-d_6) δ 168.84, 152.91, 152.46, 134.58, 132.40, 129.88, 129.67, 128.33, 127.71, 119.76, 119.51, 110.19, 28.57, 24.36, 19.96. HRMS (ESI): calcd. for $C_{32}H_{25}O_2S^+$ $[M+H]^+$ 473.1570, found .

Preparation of nanoparticles

ATX-6 (1.0 mg) was dissolved in DMSO (100 μL) and was added dropwise to vigorously stirred distilled water (2 mL). 2 hours later, the self-assembled

nanoparticles were obtained. Then, the above nanoparticles were added to stirred distilled water containing 10 mg DSPE-PEG $_{2000.}$ After another 2 hours, the solution was dialyzed for 24 h and filtered through a membrane filter (diameter = 220 nm). The concentration of **ATX-6** NPs was determined by UV-Vis spectroscopy and was quantified based on the calibration curve of **ATX-6**.

Studies on spectral properties

The UV-*vis* absorption spectra and fluorescence emissions spectra of **ATX-1**, **ATX-2**, **ATX-3**, **ATX-4**, **ATX-5**, **ATX-6** (20 μM) in different solvents and **ATX-6 NPs** (20 μM) in different pH values were measured on the UV-*vis* spectrophotometer and fluorescence spectrophotometer.

Size, morphology, and stability

DLS was applied to monitor the size of the nanoparticles in an aqueous solution, and the morphology of the nanoparticles was observed with TEM. **ATX-6 NPs** were diluted to 40 μM respectively with different pH values of PBS or DMEM containing 10% FBS. At the designated time, an aliquot of the solution was taken and monitored by DLS.

$^1O_2$ Detection in Aqueous Solution

For the $^1O_2$ detection indicated by Singlet Oxygen Sensor Green (SOSG), the stock solution of SOSG (5 mM) was diluted to 10 μM in the sample solution of **ATX-6**, **ATX-6 NPs** (10 μM) in PBS buffer. The fluorescence signal of SOSG was monitored at different time intervals in a range of 500-600 nm with the excitation wavelength at 500 nm after the solution was irradiated by an 808 nm laser. The fluorescence intensity at 533 nm was recorded to indicate the generation rate of $^1O_2$.

$O_2^{\bullet-}$ Detection in Aqueous Solution

The $O_2^{-\bullet}$ generation measurements were performed using Dihydrorhodamine 123 (DHR123) as an indicator. The stock solution of DHR 123 (5 mM) was diluted to 10

μM in the sample solution of **ATX-6** and **ATX-6 NPs** in PBS. The fluorescence signal of DHR 123 was monitored at different time intervals in a range of 500-600 nm with the excitation wavelength at 495 nm after the solution was irradiated by 808 nm laser irradiation. The fluorescence intensity at 529 nm was recorded to indicate the generation rate of $O_2^{-\bullet}$.

Detection of singlet oxygen ($^1O_2$) in vitro

1,3-Diphenlisobenzofuran (DPBF) was used as the singlet oxygen trapping agent. Briefly, 50 μL of DPBF solution in DMF (1.0 mg mL^{-1}) was added to 3.0 mL of **ATX** dyes aqueous solution or **ATX-6 NPs** with different pH values (5 μM), after exposing to an 808 nm laser for different times, and the absorbance of DPBF at 415 nm was adjusted to about 1.0. Then, the solution was exposed to an 808 nm laser and the absorption spectrums were recorded every 1 min. The slopes of absorbance of DPBF at 415 nm versus irradiation time were measured and used to compare the $^1O_2$ generation ability among **IR-1061** and **ATX** dyes.

The $^1O_2$ quantum yield of **ATX** dyes and **ATX-6** NPs in different pH values was determined using DPBF as $^1O_2$ trapper and ICG as a reference in water according to the following equation.

$$\Phi_{sam} = \frac{r_{sam}A_{ICG}}{r_{ICG}A_{sam}}\Phi_{ICG}$$

The r is the reaction rate of the DPBF with $^1O_2$ generated from **ATX** dyes, **ATX-6 NPs,** or ICG. A is the absorbance of **ATX** dyes, **ATX-6 NPs,** or ICG at 808 nm. Φ_{ICG} (0.2 %) is the $^1O_2$ quantum yield of ICG in water.[2]

Fluorescence QY measurement

The QY of **ATX** dyes was determined as follows using IR-26 as the reference (QY = 0.05 ± 0.03%).[3] IR-26 was diluted with 1,2-dichloroethane to a series of samples with their absorption intensity at 808 nm of ~0.02, ~0.04, ~0.06, ~0.08, ~0.1. The PL spectra were collected with an 880 nm LP filter to reject the excitation light

(808 nm). Then the emission spectra were integrated in the 850–1400 nm region. The same procedures were performed for the samples in water and DMSO too. The obtained emission integration was plotted against the absorption intensity and fitted into a linear relationship. The QY calculation equation was as follows: [4]

$$QY_{sam} = QY_{ref} \cdot \frac{S_{sam}}{S_{ref}} \cdot \left(\frac{n_{sam}}{n_{ref}}\right)^2$$

where QY_{sam} is the QY of the nanoparticles in 850–1400 nm, QY_{ref} is the QY of IR-26 (0.05 ± 0.03% in dichloroethane), S_{sam} and S_{ref} are the slopes obtained by linear fitting of the integrated emission spectra of the nanoparticles (850–1400 nm), and IR-26 (850–1400 nm) against the absorbance at 808 nm, n_{sam} and n_{ref} are the refractive indices of DMSO, H_2O and dichloroethane, respectively.

Computational Methods

Density functional theory (DFT) and time-dependent DFT (TD-DFT) were employed to rationalize the properties of designed **ATX** dyes. Geometry optimizations in the ground state were carried out with B3LYP functional and 6-311G basis set. The singlet and triplet energies as well as corresponding oscillator strengths were calculated with time-dependent density functional theory (TD-DFT) at the wB97XD/6-31G level. All the quantum calculations of the dyes were carried out with the Gaussian 09, except stated otherwise. The spin-orbital coupling (SOC) between the singlet and triplet excited states was calculated with ORCA 5.0 and the input files of ORCA were generated by Multiwfn.[5]

Cell Culture

L02 cells, 4T1 cells, and MCF-7 cells were purchased from Nanjing Keygen Biotech (Nanjing, China), the cells were cultured in a medium containing Dulbecco's Modified Eagle's Medium (DMEM), 10% FBS, and 1% penicillin-streptomycin in a CO_2 incubator (37 °C with 5% CO_2).

Cytotoxicity in Dark

L02 cells, 4T1 cells, and MCF-7 cells were separately seeded in a 96-well plate with a density of 5×10^5 cells per well. After 24 h incubation, different concentrations of **ATX-6 NPs** (0, 0.5, 1, 2, 4, 6, 8, 10, and 20 μM) were added to the wells and incubated with cells for another 6 h. After that, the medium was removed, and cells were washed twice with 100 μL PBS buffer. Subsequently, 100 μL fresh medium and 10 μL CCK-8 were added, followed by incubation for 1 hour. Finally, the absorbance values at 450 nm were recorded on a microplate reader.

The relative cell viability was calculated according to the following formula:

Cell viability (%) = $(OD_{sample} - OD_{background})/(OD_{control} - OD_{background}) \times 100\%$

***In vitro* Photodynamic Therapy**

L02 cells, 4T1 cells, and MCF-7 cells were separately seeded on 96 well plates (5×10^5 cells / well) and cultured for 24 h. Then the medium was discarded and different concentrations of **ATX-6 NPs** (0, 0.5, 1, 2, 4, 6, 8, 10, and 20 μM) dispersed in 100 μL fresh medium with different pH values were added to the wells. The cells were incubated for 6 h and then received or not the 808 nm (1.5 W cm^{-2}) laser for 3 min. 10 μL CCK-8 was added, followed by incubation for 1 hour, and the absorbance values at 450 nm were recorded on a microplate reader.

Intracellular $^1O_2$ detection

2′,7′-Dichlorofluorescin diacetate (DCFH-DA) was used to evaluate the generation of singlet oxygen in 4T1 cells. Briefly, 4T1 cells were seeded in confocal dishes at a density of 3×10^5 cells per dish and cultured for 12 h. Then, different concentrations of **ATX-6 NPs** (0, 4, and 6 μM) containing different pH DMEM medium were added and incubated for another 4 h. Then the media was removed and 4T1 cells were washed with cold PBS three times, and incubated with DCFH-DA working solution for 30 min. For fluorescence imaging, 4T1 cells were irradiated with an 808 nm laser (1.5 W cm^{-2}) for 3 min and stained with 4′,6-diamidino-2-phenylindole (DAPI) and observed by CLSM. the excitation wavelength of 426-466 nm and the emission collection wavelength was 500-550 nm.

Live/dead Cell Staining Assay

4T1 cells were seeded in the CLSM dish and cultured for 24 h, **ATX-6 NPs** (0, 4, and 6 μM) were then added into the cell culture medium with different pH values and incubated continuously for another 6 h. After that, the cells were irradiated with or without an 808 nm laser (1.5 W cm^{-2}, 3 min) and cultured at 37 °C for another 1 h. Rinsed with cold PBS and stained by 2 μM calcein acetoxymethyl ester (Calcein-AM) and 8 μM propidium iodide (PI) for 30 min, CLSM was applied to observe the green fluorescence of Calcein-AM and red fluorescence of PI indicating live and dead cells, respectively. Conditions: excitation wavelength: 495 nm for Calcein-AM, 530 nm for PI; emission filter: 511-551 nm for Calcein-AM, 573-613 nm for PI.

Scratch-Wound Healing Assay

4T1 cells were seeded into a 24-well plate at a density of 4×10^5 cells per well and cultivated for 24 h. A 10 μL pipette tip was used to make a straight scratch gently at the center of the well and washed with PBS twice. After 0, 12, and 24 hours of cultivation at 37 °C, horizontal migration of the cells was measured by the microscope after being treated with different concentrations of **ATX-6 NPs** (0, 4, and 6 μM) containing different pH DMEM medium with or without 808 nm laser irradiation (1.5 W cm^{-2}, 5 min).

Flow cytometer analysis.

4T1 cells were seeded in 6-well plates at a density of 4×10^5 cells per well and cultivated for 24 h, **ATX-6 NPs** (0, 4, and 6 μM) were then added into the cell culture medium with different pH values and incubated continuously for another 6 h. After that, the cells were irradiated with or without an 808 nm laser (1.5 W cm^{-2}, 3 min) and cultured at 37 °C for another 1 h. Then, the cells were washed with cold PBS, digested by trypsinization without EDTA, and collected by centrifuge. Next, the cells obtained were resuspended in PBS and stained with Annexin VAlexa Fluor 488/PI apoptosis detection kit according to the manufacturer's instructions. Finally, the 4T1

cell suspension was examined with a FAATX Calibur flow cytometer.

Animals and Tumor-Bearing Mouse Model

Female BALB/c mice, 6 weeks of age, were purchased from the Qinglongshan Animal Breeding Farm (Nanjing, China). All animal experiments were performed by the Guidelines for Care and Use of Laboratory Animals of China Pharmaceutical University and experiments were approved by China Pharmaceutical University Animal Care and Use Committee.

To establish the breast tumor model, 4T1 breast cancer cells (1×10^6) were injected subcutaneously on the left flank of the mice. The tumor size was measured by a slide caliper every day after the injection. After about 7 days, mice with tumor volumes at about 100 mm^3 were used subsequently. The tumor volumes were measured every other day using a caliper and calculated using the following formula:

$$Volume = (1/2 \times Tumor\ length \times (Tumor\ width)^2)$$

***In vivo* fluorescence imaging**

4T1 tumor-bearing nude mice were used for in vivo NIR-I fluorescence imaging. When the tumor grew to ~100 mm^3, the mice were administered **ATX-6** or **ATX-6 NPs** (20 μM, 100 μL) through intravenous injection. The animal imaging system (IVIS Lumina III, Perkin Elmer) was applied for fluorescence imaging mice at various time points after injection. After which, the 24 h post-administration mice were sacrificed while the tumors and major organs (heart, liver, spleen, lung, and kidneys) were subjected to ex vivo fluorescence imaging. Additionally, the fluorescence images were analyzed by the Living Image software.

For NIR-II fluorescence imaging, the 4T1 tumor-bearing nude mice were administered **ATX-6** or **ATX-6 NPs** (20 μM, 100 μL) via the tail vein. Then the mice were imaged at different time points through a commercial measurement purchased from Suzhou NIR OptiATX Technologies CO., Ltd. (Dali-IGS 600), with the long pass (LP) filter of 900nm, 1000 nm, and 1100nm. After 24 h post-administration, mice were sacrificed while the tumors and major organs (heart, liver, spleen, lung,

and kidneys) were subjected to ex vivo fluorescence imaging.

Standard *in vitro* hemolysis assay

The red blood cells (RBC) from BALB/c nude mice blood were concentrated by centrifugation at 3000 rpm for 5 min and washed with saline. Subsequently, **ATX-6 NPs** with different concentrations (5, 10,20, 30, and 50 μM) were added into the RBC suspension and mixed completely. The mixtures were further incubated for 3 h at 37 ℃. Finally, the suspension supernatant was concentrated by centrifugation (3000 rpm, 5 min). After being photographed, the supernate was moved to a 96-well plate and measured the absorption at 545 nm. The physiological saline and distilled water were used as negative and positive controls. The hemolytic percentage (HP) value was obtained using the following equation:

$$HP(\%) = \frac{OD_{sample} - OD_{negative}}{OD_{positive} - OD_{negative}}$$

In which OD_{sample}, $OD_{negative}$, and $OD_{positive}$ represent the absorbance of RBC treated with **ATX-6 NPs**, saline, and distilled water.

***In vivo* phototherapeutic study**

The 4T1 tumor-bearing mice were randomly divided into 5 groups (n = 5 for each group) when the inoculated tumor volumes reached about 100 mm^3: 1) Saline (100 μL), 2) Saline (100 μL) + laser, 3) **ATX-6** (20 μM, 100 μL) + laser, 4) **ATX-6 NPs** (20 μM, 100 μL), and 5) **ATX-6 NPs** (20 μM, 100 μL) + laser, respectively. The 808 nm laser (1.5 W cm^{-2}) was used to irradiate the tumor for 10 min at 8 h post-injection. The tumor volumes and body weight were measured every three days during the 21-day treatment period. Besides, the survival of the mice was also recorded during treatment.

Histological analyses

After 21 days of treatment, the mice involved in the control and experimental group were sacrificed. The tumors, hearts, livers, spleens, lungs, and kidneys were

collected and fixed in 4% paraformaldehyde, embedded in paraffin, sectioned at 5 μm thickness, and stained with H&E for histopathological evaluation.

Biosafety Evaluation

Blood routine examination and serum analysis were carried out by collecting the blood and serums of healthy female BALB/c mice 3 days post-administration with saline (100 μL), **ATX-6** (100 μL, 20 μM), and **ATX-6 NPs** (100 μL, 20 μM) (n = 3). White blood cell (WBC) counts, red blood cell (RBC), hemoglobin (HGB), hematocrit (HCT), mean corpuscular volume (MCV), mean corpuscular hemoglobin (MCH), mean corpuscular hemoglobin concentration (MCHC), red blood cell volume distribution width (RDW) and platelets (PLT) were examined by an automatic blood cell analyzer (Chemray 800, Shenzhen Rayto Life Technology). For biochemical blood analysis, alanine aminotransferase (ALT), transaminase (AST), blood urea nitrogen (BUN), creatinine (CREA), and uric acid (UA) were measured.

Statistical Analysis

All data were expressed in this research as mean result ± standard deviation (s.d.). All figures shown in this article were obtained from three or more independent experiments with similar results unless specifically mentioned. The significance of differences among groups was evaluated with one-way ANOVA and a Student's t-test (*$P < 0.05$, **$P < 0.01$, ***$P < 0.001$, and ****$P < 0.0001$).

Supplementary Tables and Figures

Table S1. Photophysical for **ATX** PSs

PSs	λ_{abs}/nm	λ_{em}/nm	$\varepsilon*10^5$ $M^{-1}cm^{-1}$	Φ_F	Φ_Δ
ATX-1	825	946	0.8	0.99%	16.5%
ATX-2	837	933	0.82	2.53%	23.7%
ATX-3	820	933	0.35	0.40%	9.3%
ATX-4	841	939	1.60	2.24%	19.0%
ATX-5	790	923	0.12	0.17%	35.9%
ATX-6	757	923	1.34	0.24%	38.2%

Table S2. DFT calculations for **ATX** PSs

PSs	LUMO [eV]	HOMO [eV]	E_g [eV]	E_{s1} [eV]	E_{T1} [eV]	ΔE_{st} [eV]
ATX-1	-3.17	-5.21	2.04	1.78	0.92	0.86
ATX-2	-3.12	-5.11	1.99	1.82	0.97	0.85
ATX-3	-3.20	-5.08	1.88	1.71	0.86	0.85
ATX-4	-3.16	-4.97	1.81	1.69	0.83	0.86
ATX-5	-3.32	-5.41	2.09	1.94	1.01	0.93
ATX-6	-3.25	-5.34	2.09	1.97	1.03	0.94

Table S3. The dosage used in the hemocompatibility assay

Concentration	5% Red Cell Suspension	Normal Saline	Sample for Test	Total Volume	Hemolysis Ratio of ATX-6	Hemolysis Ratio of ATX-6 NPs
5 μM	200 μL	994 μL	6 μL	1200 μL	1.13%	0.89%
10 μM	200 μL	988 μL	12 μL	1200 μL	1.26%	1.04%
20 μM	200 μL	976 μL	24 μL	1200 μL	1.64%	1.32%
30 μM	200 μL	964 μL	36 μL	1200 μL	1.78%	1.53%
40 μM	200 μL	952 μL	48 μL	1200 μL	2.03%	1.92%

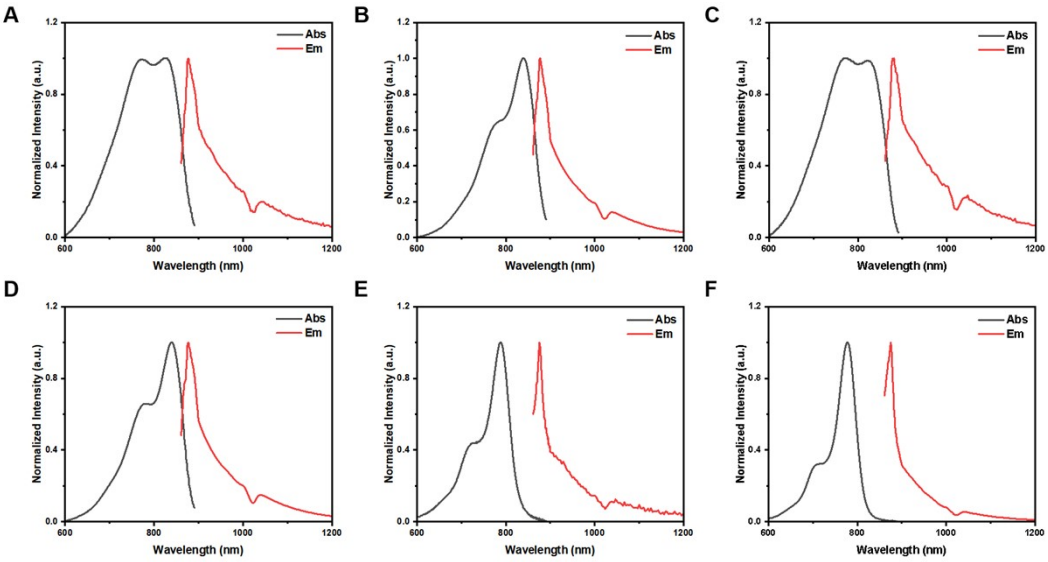

Figure S1. Normalized absorption and emission spectra of **ATX** PSs in DCM.

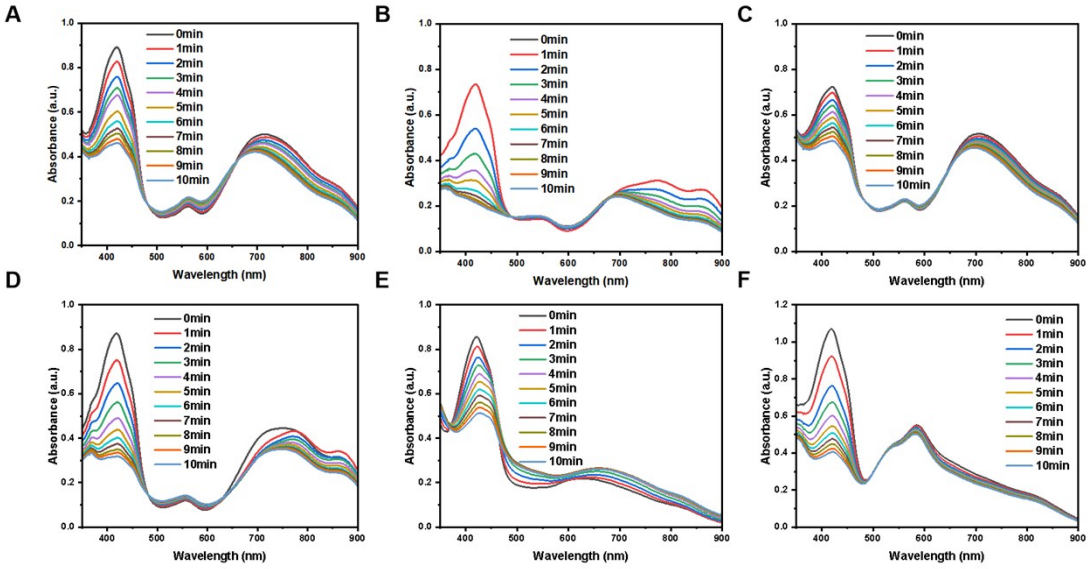

Figure S2. Singlet oxygen generation of **ATX-1** ~ **ATX-6** using DPBF as a probe.

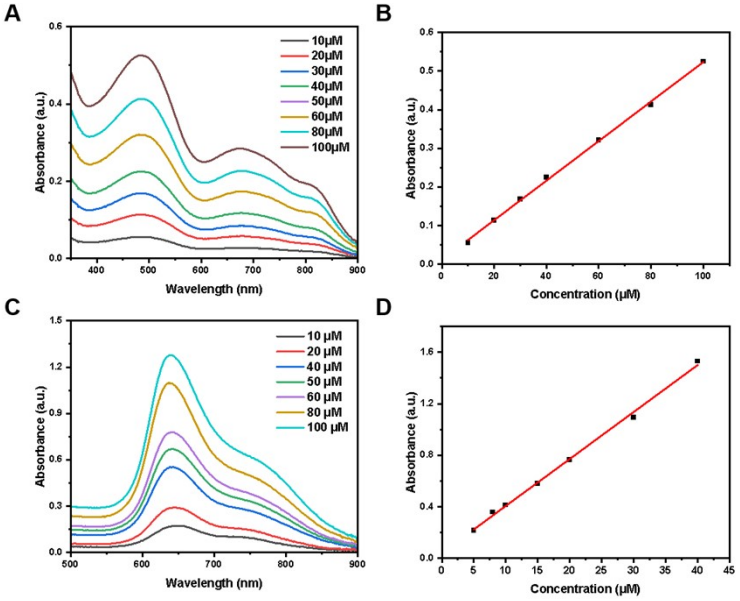

Figure S3. A) UV-vis spectra of **ATX-5** at different concentrations. B) Linear fitting of the absorbance for **ATX-5**. C) UV-vis spectra of **ATX-6** at different concentrations. D) Linear fitting of the absorbance for **ATX-6**.

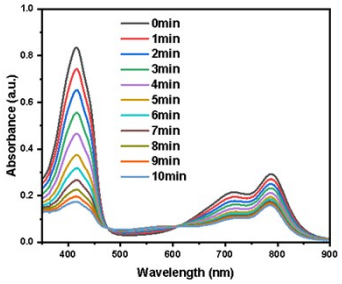

Figure S4. $^1O_2$ generation of **ATX-6 NPs** (20 μM) under the pH value of 6.5 using DPBF as the probe.

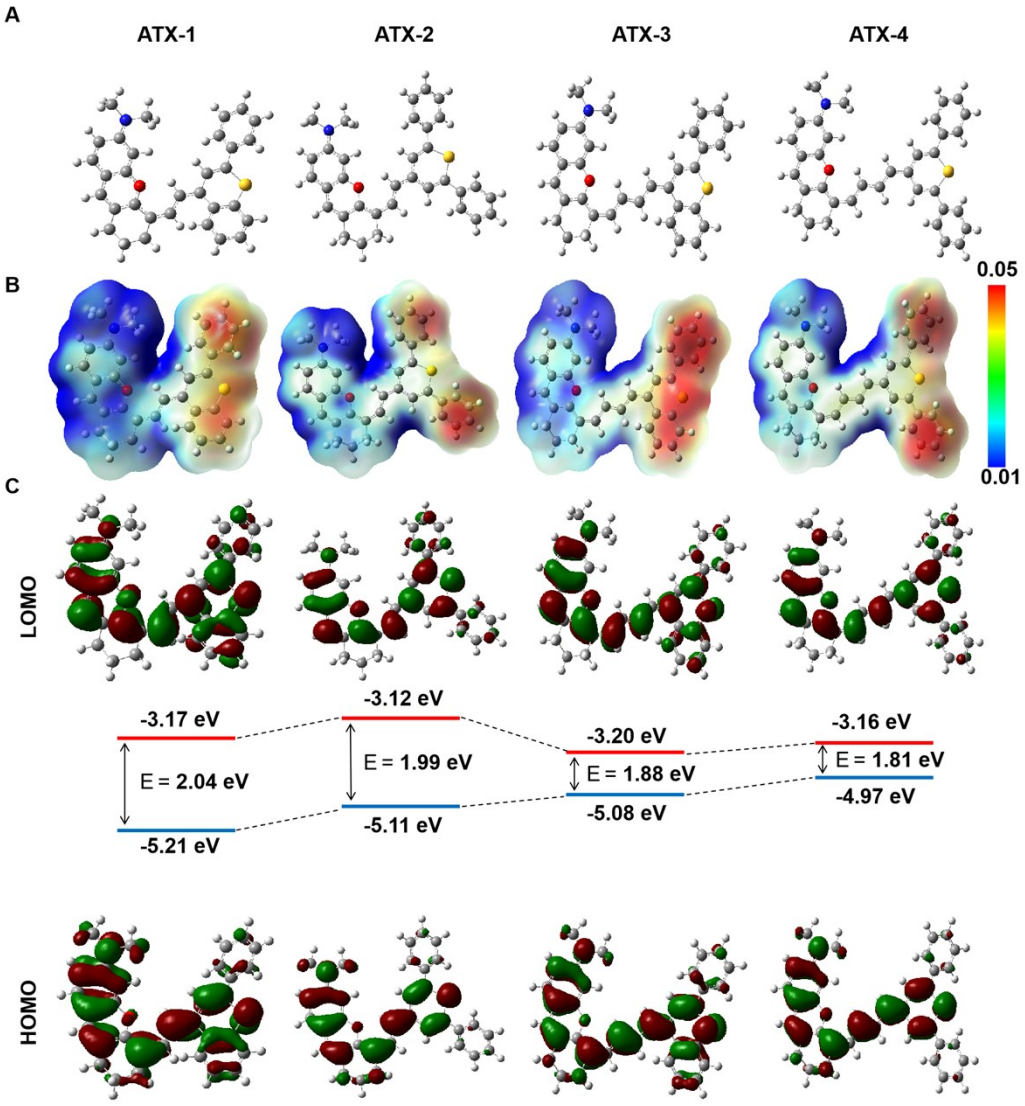

Figure S5. A) Optimized geometries B) ESP diagram, C) illustration of the HOMO

and LUMO energy levels of **ATX-1** ~ **ATX-4**.

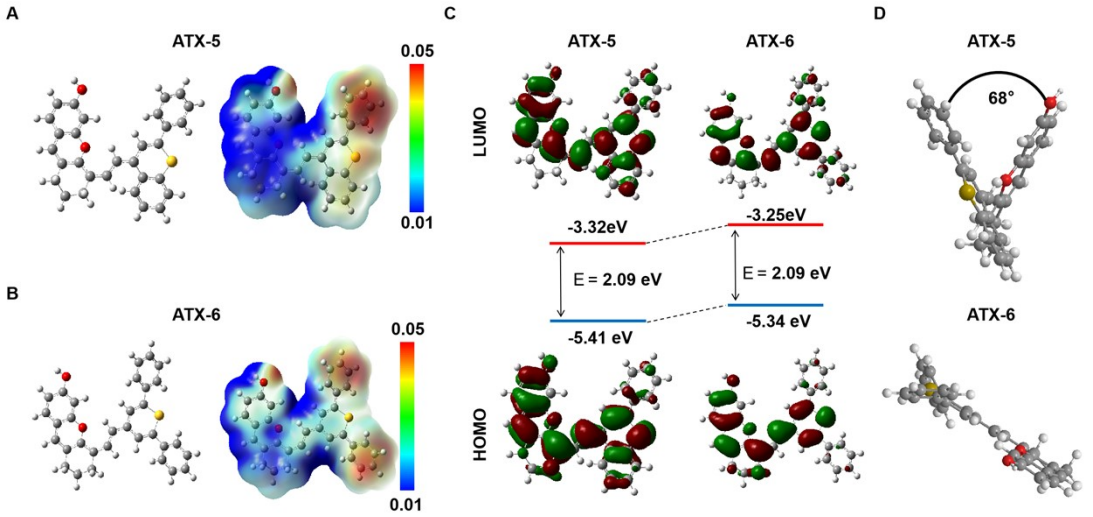

Figure S6. A, B) Optimized geometries and ESP diagram of **ATX-5** and **ATX-6**. C) illustration of the HOMO, LUMO energy levels, and D) side view of **ATX-5** and **ATX-6**, based on TDDFT calculations at the B3LYP/6–311 G(d,p) level.

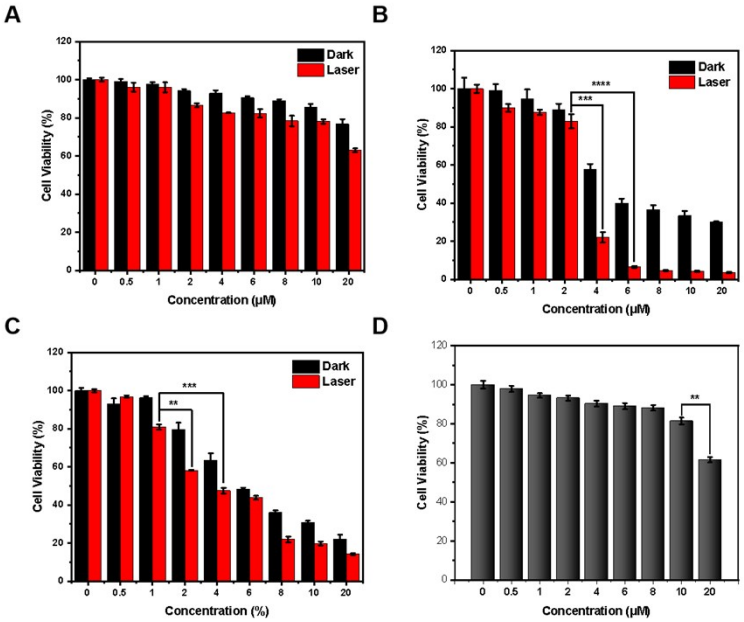

Figure S7. In vitro cell cytotoxicity study. A) L02 cells, B) MCF-7 cells, and C) 4T1 cells treated with different concentrations of **ATX-6 NPs** with or without the 808 nm Laser irradiation for 3 min (1.5W cm^{-2}). D) 4T1 cells received various concentrations of **ATX-6** without an 808 nm laser.

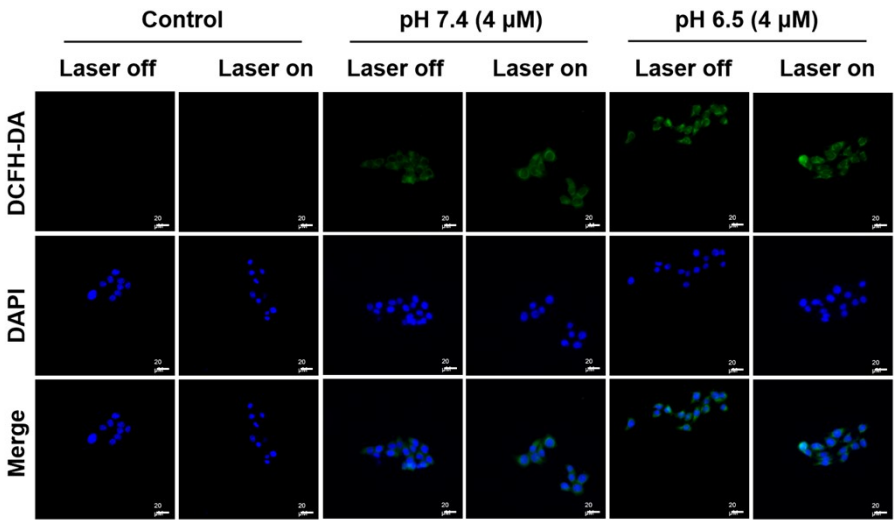

Figure S8. Detection of intracellular ROS generation by DCFH-DA in 4T1 cells after various treatments of **ATX-6 NPs** in pH 7.4 and pH 6.5 conditions with or without 808 nm laser irradiation (1.5W cm^{-2}, 3 min). Scale bar: 20 μm.

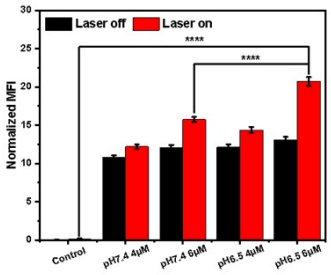

Figure S9. Quantitative fluorescence intensity for the intracellular ROS generation by DCFH-DA (green channel) after 4T1 cells incubated with **ATX-6 NPs** (4 μM and 6 μM) in different pH values. The data were presented as mean ± SD (n = 3), *P < 0.05, **P < 0.01, ***P < 0.001, and ****P < 0.0001.

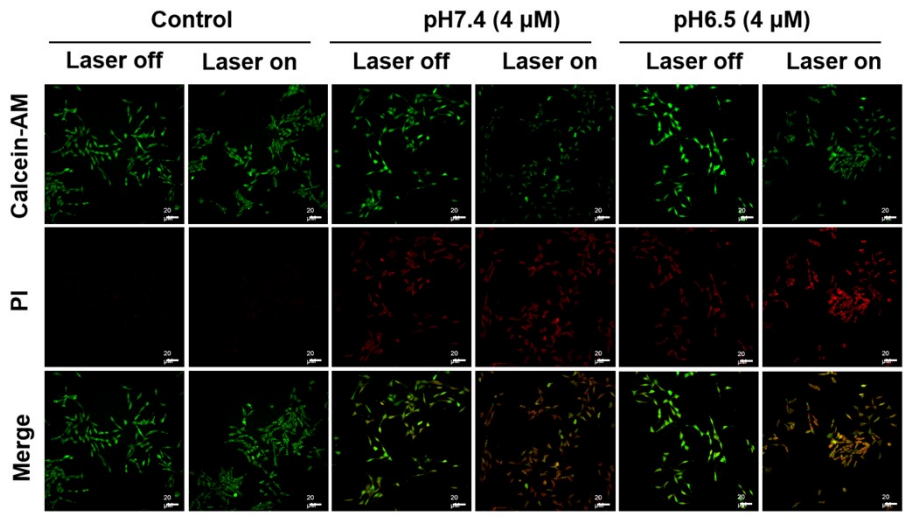

Figure S10. Fluorescence images of Calcein AM (green, live cells) and propidium iodide (red, dead cells) costained 4T1 cells treated with **ATX-6 NPs** in pH7.4 and pH6.5 with or without 808 nm laser irradiation (1.5W cm^{-2}, 3 min). Scale bar: 20 μm.

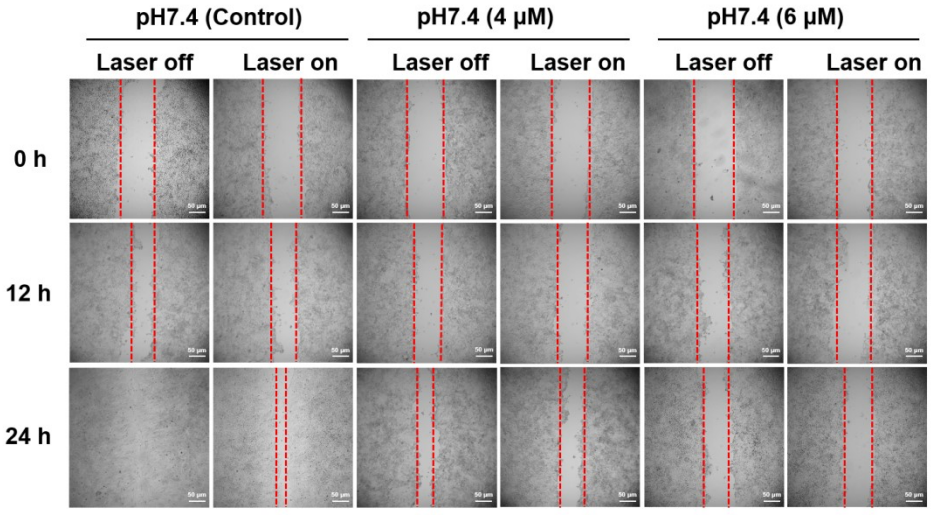

Figure **S11.** Scratch healing assessment of 4T1 cells received PBS or **ATX-6 NPs** in pH7.4 condition. Scale bar: 50 μm.

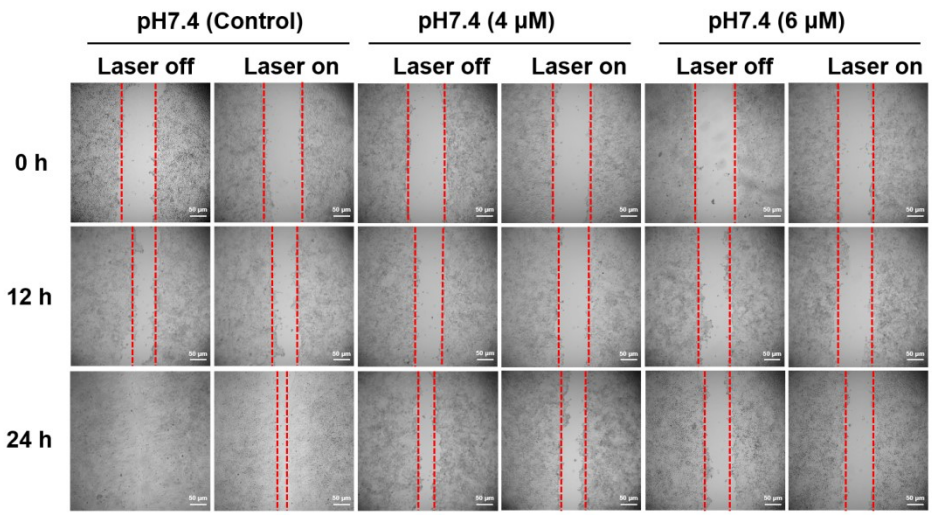

Figure S12. Scratch healing assessment of 4T1 cells received PBS or **ATX-6 NPs** in pH 6.5 condition. Scale bar: 50 μm.

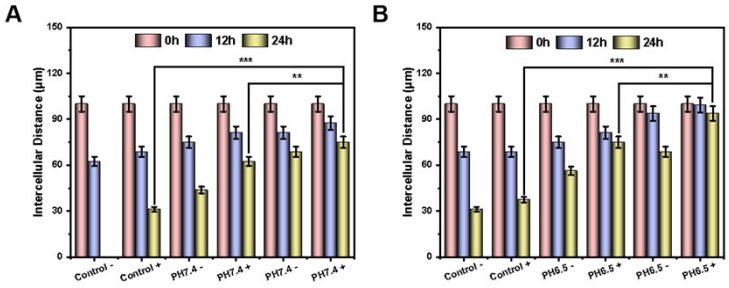

Figure S13. Quantification cell distance for 4T1 cells incubated under A) pH7.4 and B) pH6.5 after scratching. The data were presented as mean ± SD (n = 3), *P < 0.05, **P < 0.01, ***P < 0.001, and ****P < 0.0001.

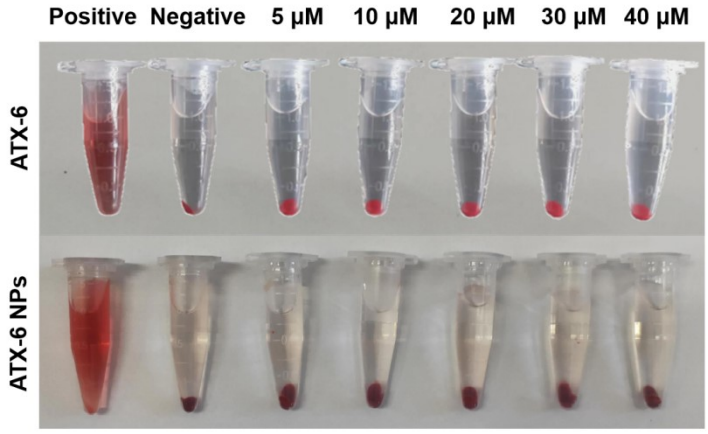

Figure S14. In vitro hemolysis assay of **ATX-6** and **ATX-6 NPs**.

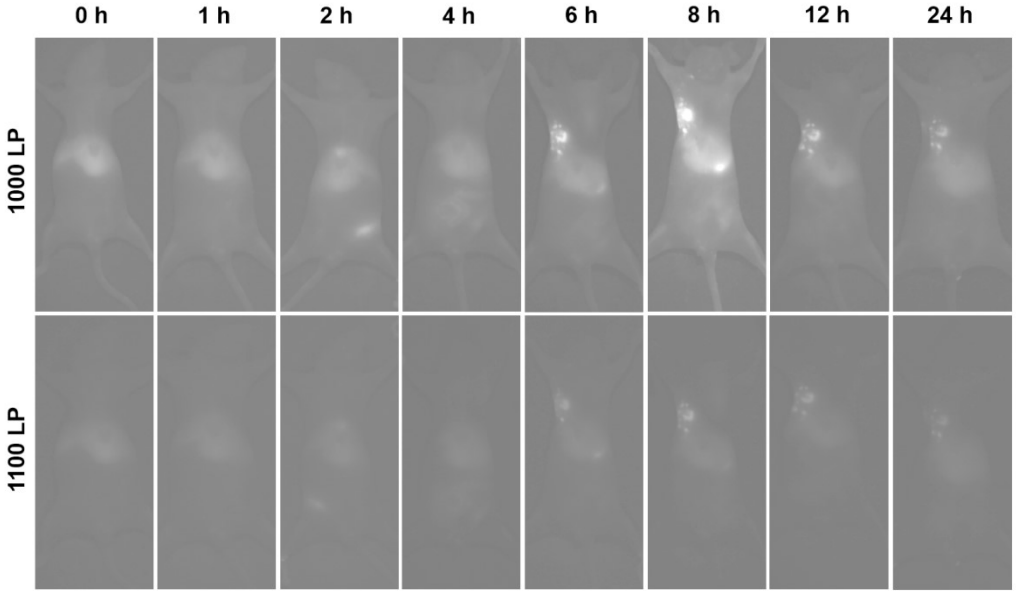

Figure S15. *In vivo* NIR-II fluorescence images under different filters of 4T1-tumor-bearing mice at different time points after intravenous injection of 100 μL **ATX-6 NPs** (6 μM).

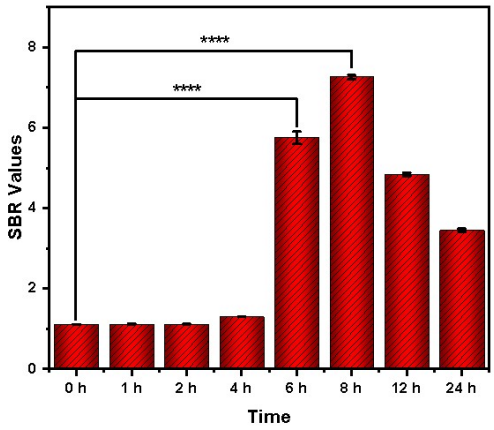

Figure S16. Signal-to-background ratio (SBR) values of **ATX-6 NPS** at different times (900 LP). Data are means ± SD. *P < 0.05, **P < 0.01, ***P < 0.001, and ****P < 0.0001.

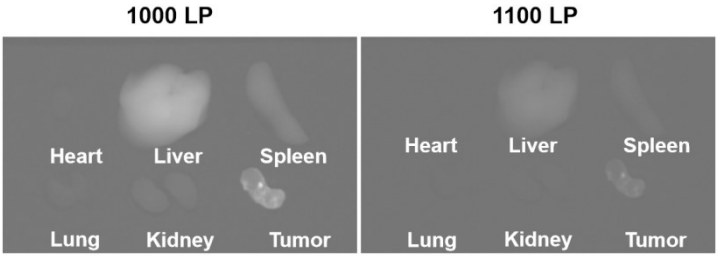

Figure S17. The bio-distribution of **ATX-6 NPs** in tumor, heart, liver, spleen, lung, and kidney 24 h after intravenous injection with different filters of NIR-II fluorescence imaging system.

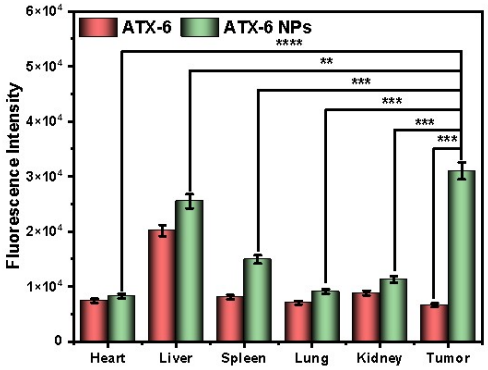

Figure S18. Quantification fluorescence intensity of isolated main organs and tumor in 4T1 tumor-bearing mice under NIR-II fluorescence imaging system (900nm filter) 24 hours after injection of **ATX-6** and **ATX-6 NPs** through the tail vein. Data are means ± SD. *P < 0.05, **P < 0.01, ***P < 0.001, and ****P < 0.0001.

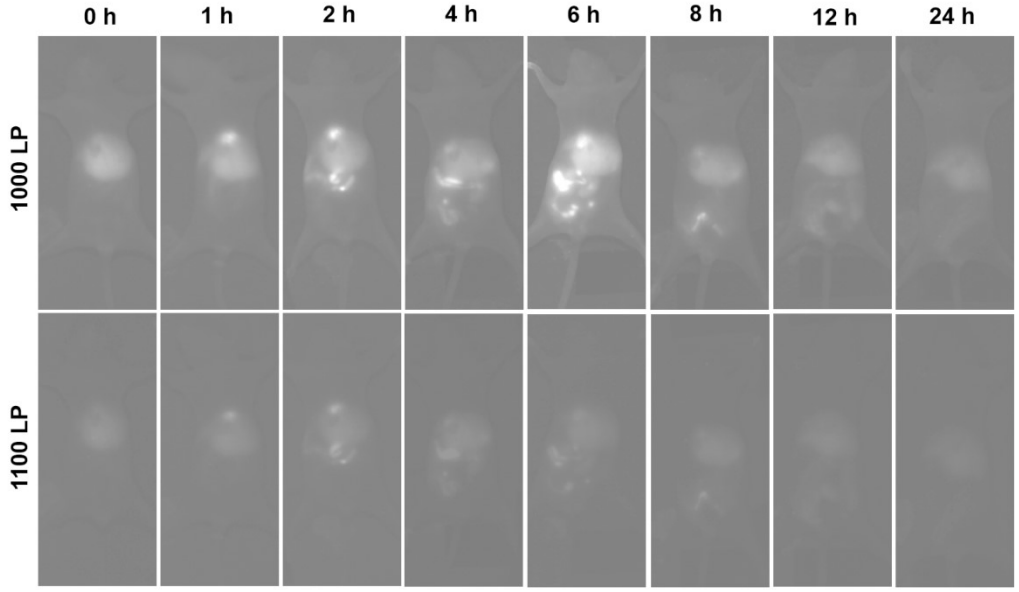

Figure S19. *In vivo* NIR-II fluorescence images under different filters of 4T1-tumor-bearing mice at different time points after intravenous injection of 100 μL **ATX-6 NPs** (6 μM).

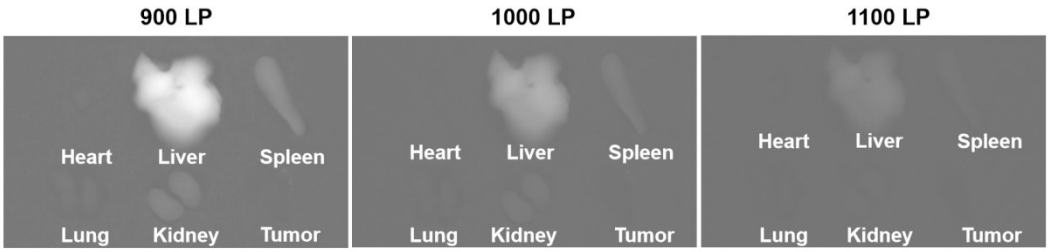

Figure S20. The bio-distribution of **ATX-6** in tumor, heart, liver, spleen, lung, and kidney 24 h after intravenous injection with different filters of NIR-II fluorescence imaging system.

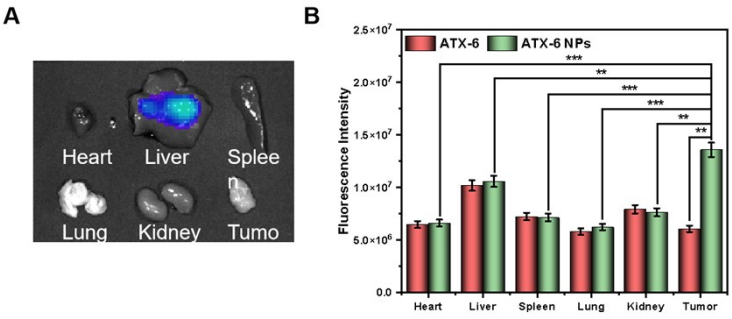

Figure S21. A) *Ex vivo* NIR-I fluorescence images of major organs and tumors dissected from mice after 24 h post-injection of **ATX-6**. B) Quantification fluorescence intensity of isolated main organs and tumor in 4T1 tumor-bearing mice under NIR-II fluorescence imaging system (900nm filter) 24 hours after injection of **ATX-6** and **ATX-6 NPs** through the tail vein. Data are means ± SD. *P < 0.05, **P < 0.01, ***P < 0.001, and ****P < 0.0001.

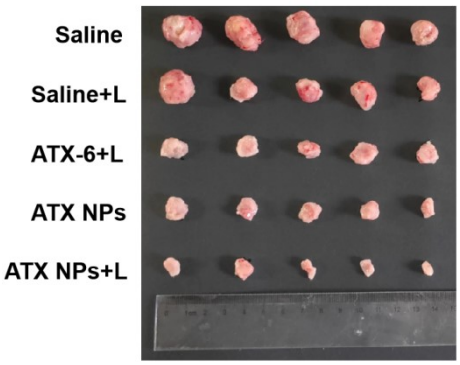

Figure S22. Representative photos of the sacrificed tumor on the 21st day.

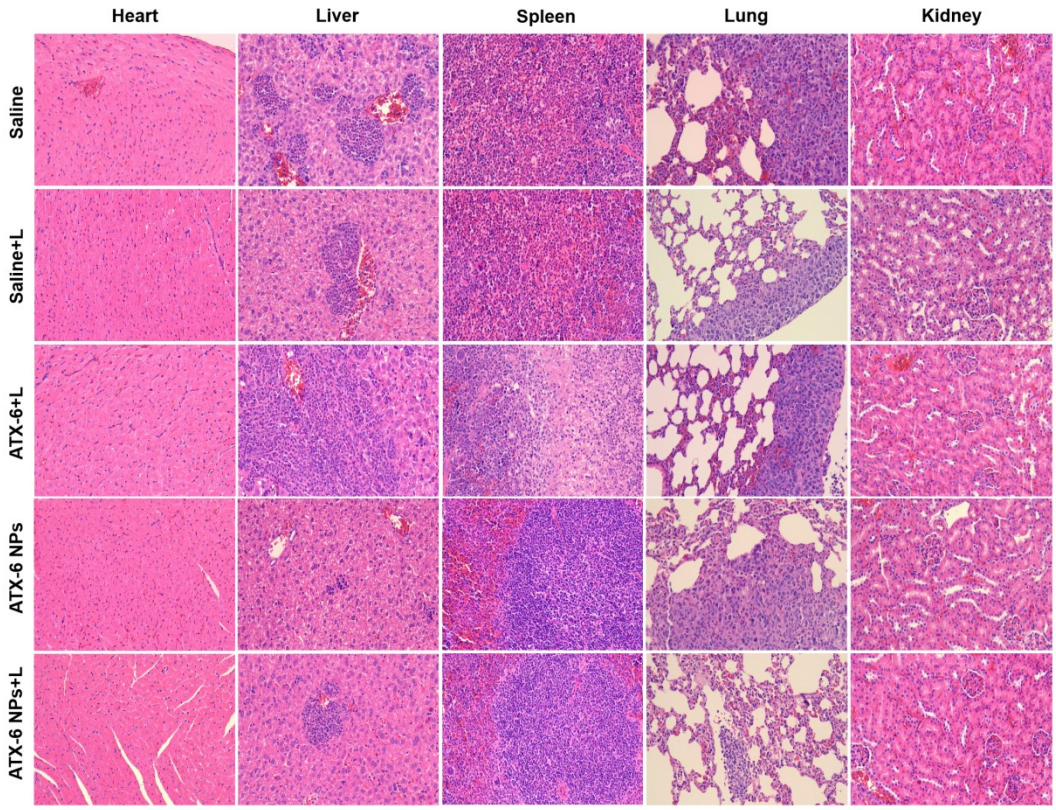

Figure S23. H&E staining of main organs and tumors from mice at 21 days after various treatments. Scale bar: 100 μm.

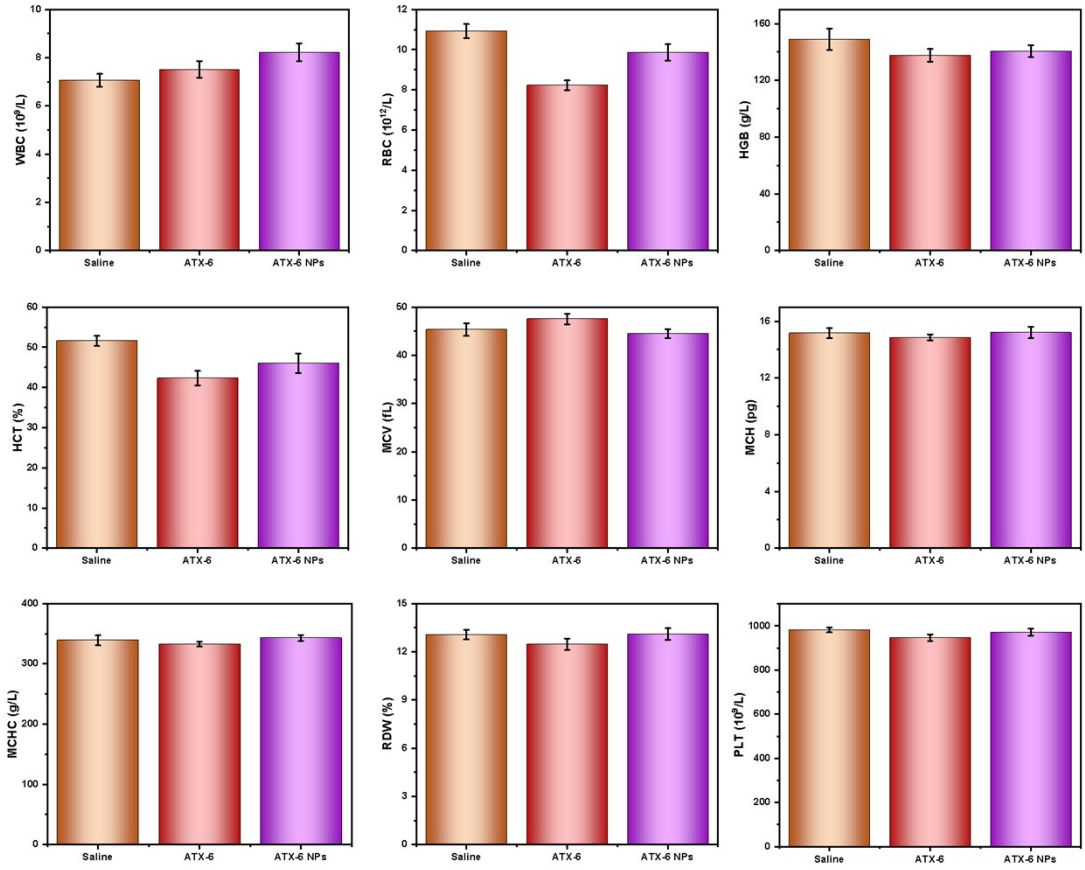

Figure S24. Hematology analysis of the mice in saline, **ATX-6**, and **ATX-6 NPs** 3 days post-injection (n = 3). Data are means ± SD.

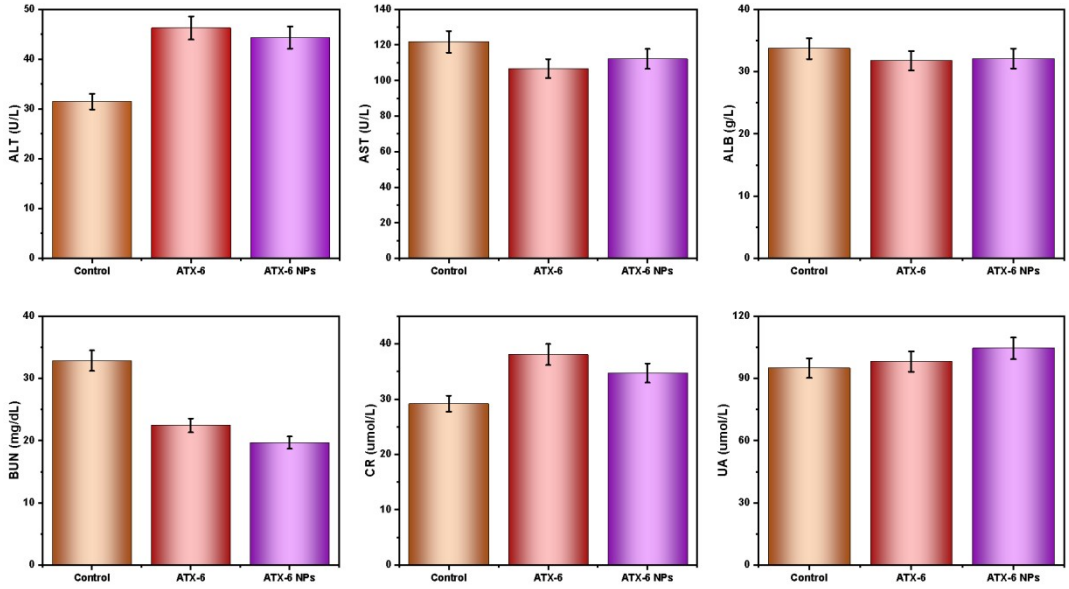

Figure S25. Blood biochemistry analysis of the mice in saline, **ATX-6**, and **ATX-6 NPs** 3 days post-injection (n = 3). Data are means ± SD.

NMR and HR-MS Spectra

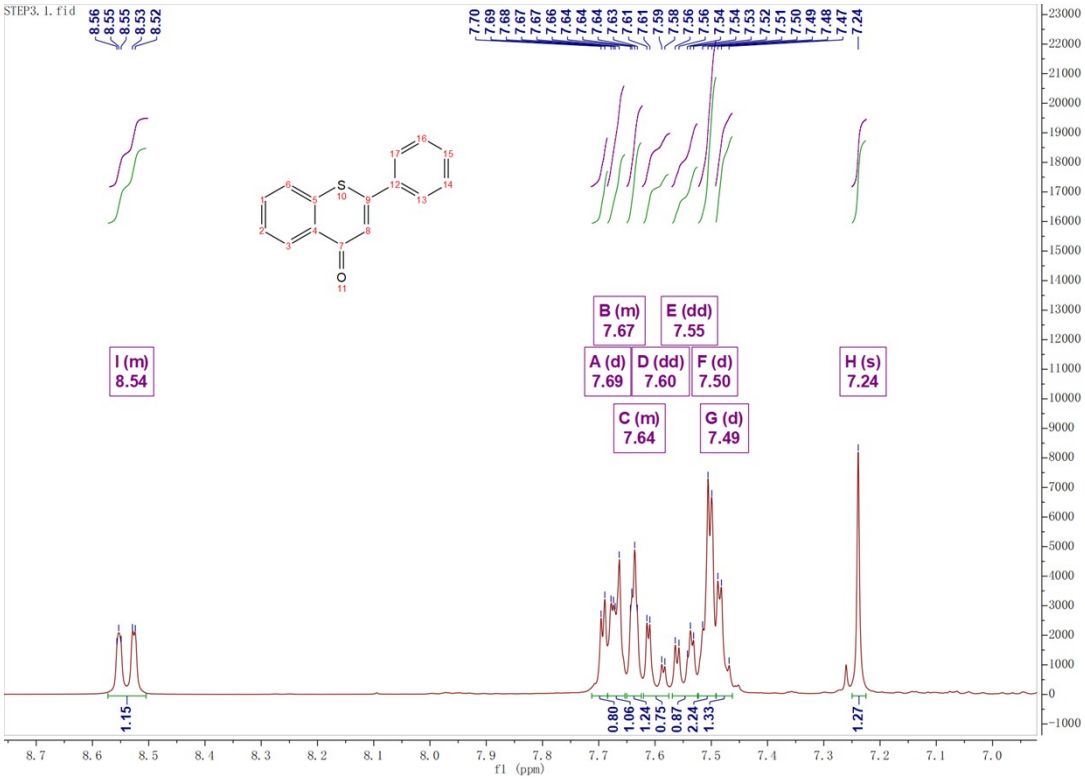

Figure S26. ^{1}H NMR spectrum of **1**.

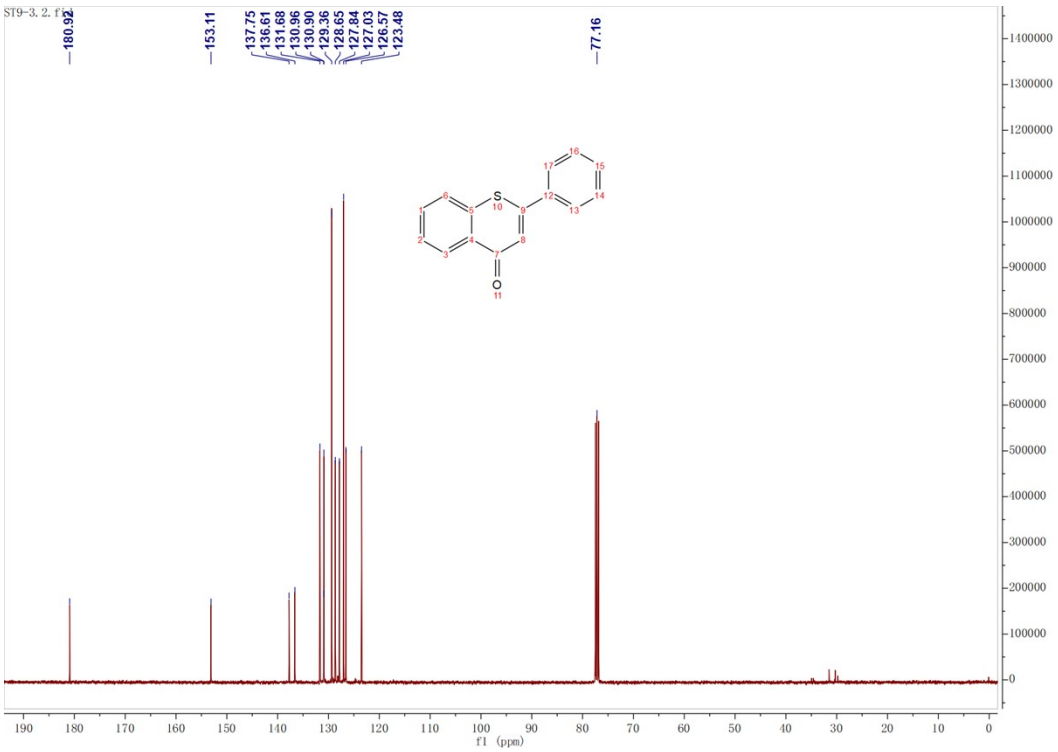

Figure S27. ^{13}C NMR spectrum of **1**.

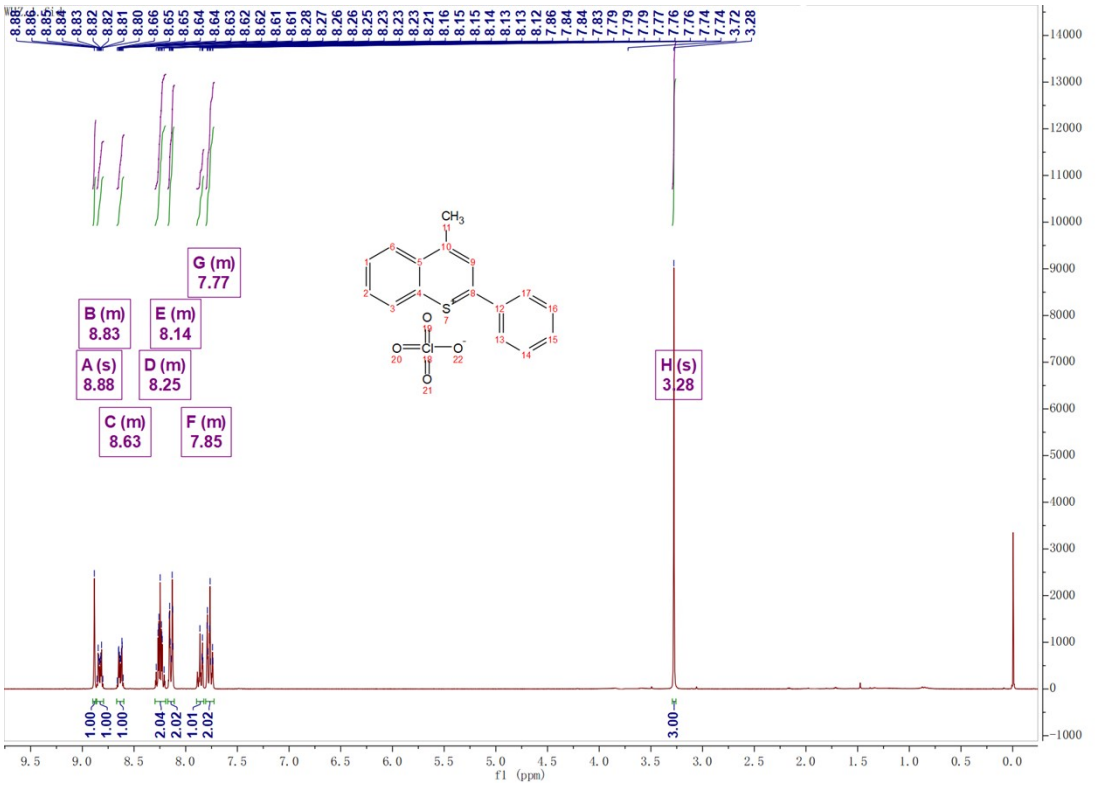

Figure S28. ^{1}H NMR spectrum of **2**.

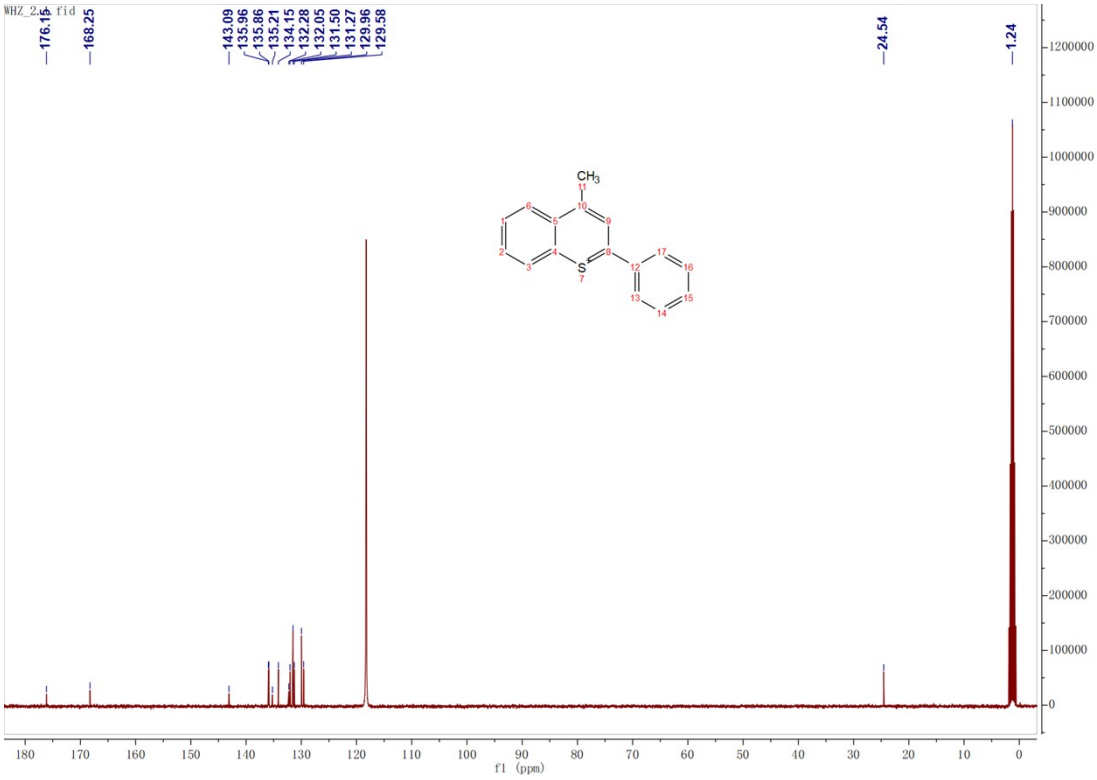

Figure S29. ^{13}C NMR spectrum of **2**.

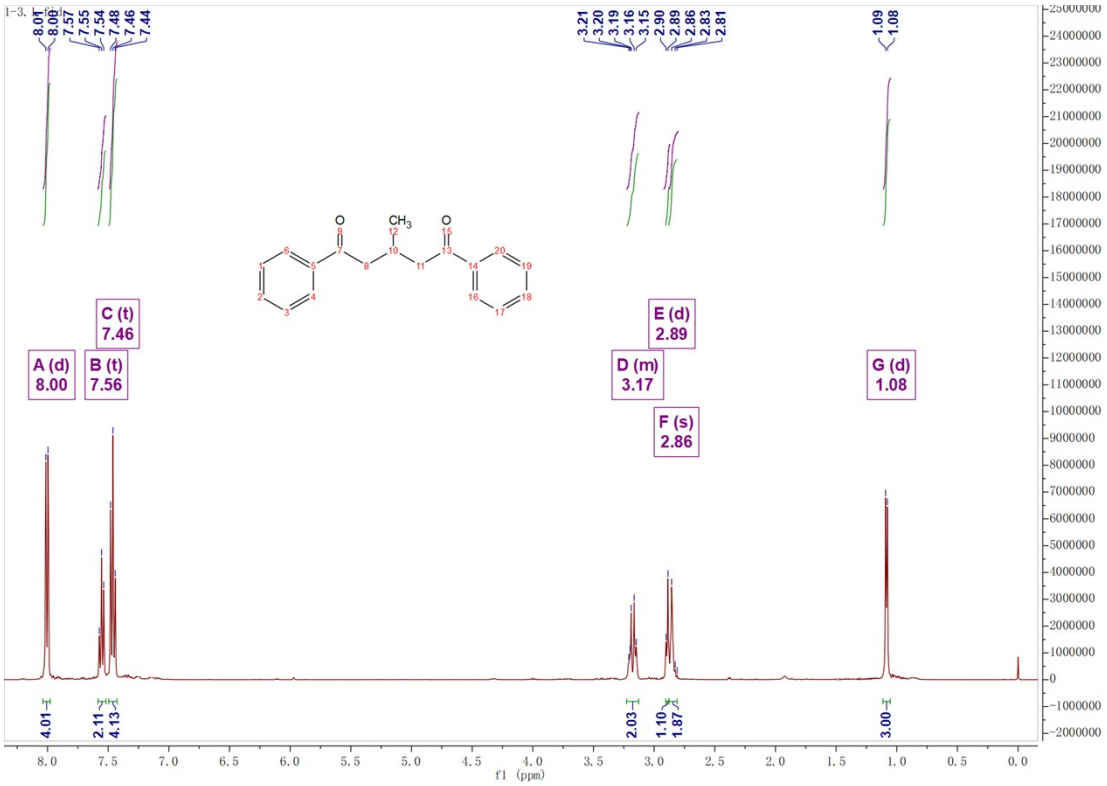

Figure S30. ^{1}H NMR spectrum of **3**.

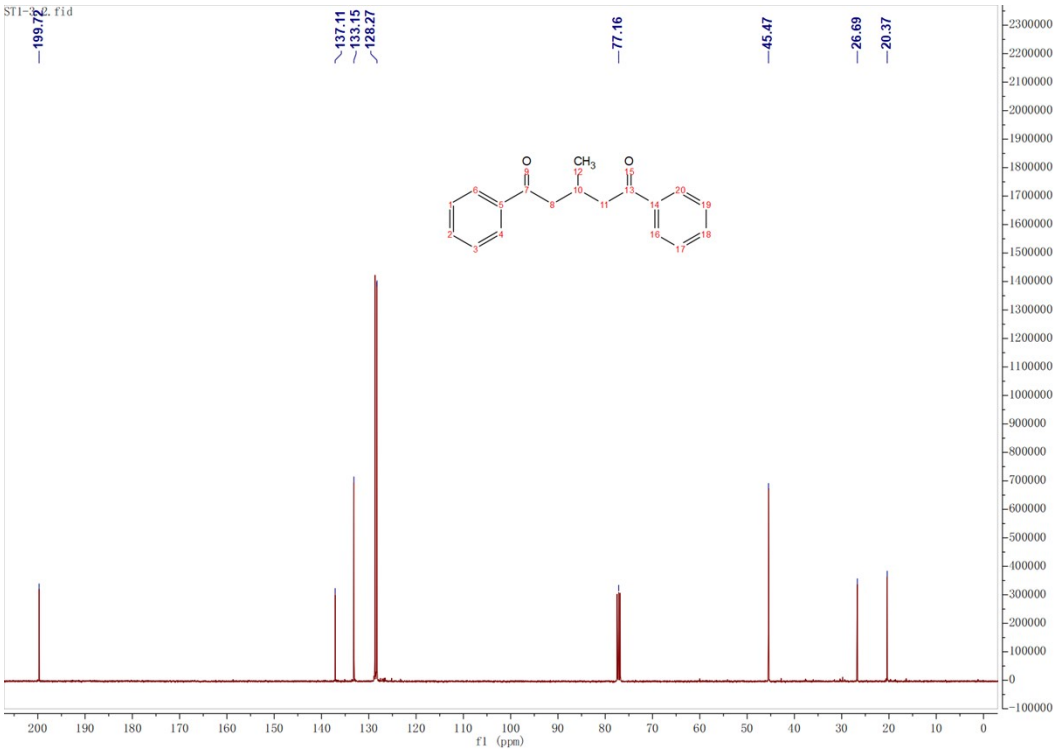

Figure S31. ^{13}C NMR spectrum of **3**.

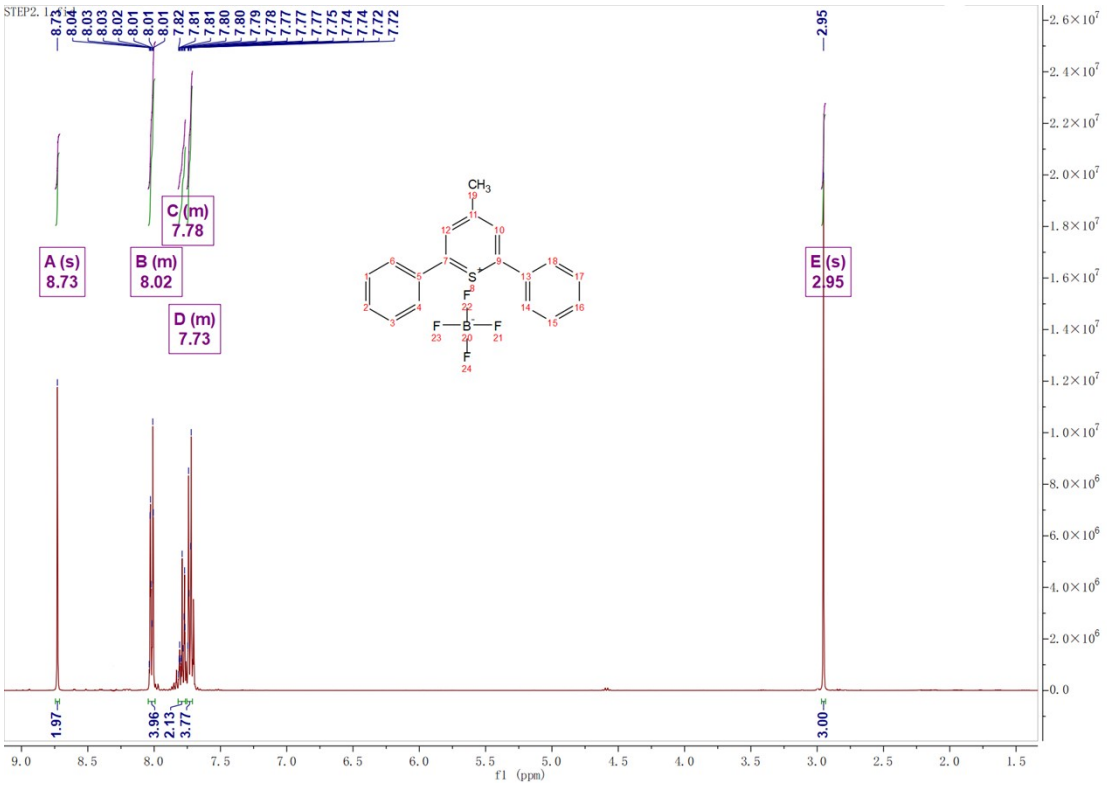

Figure S32. ^{1}H NMR spectrum of **4**.

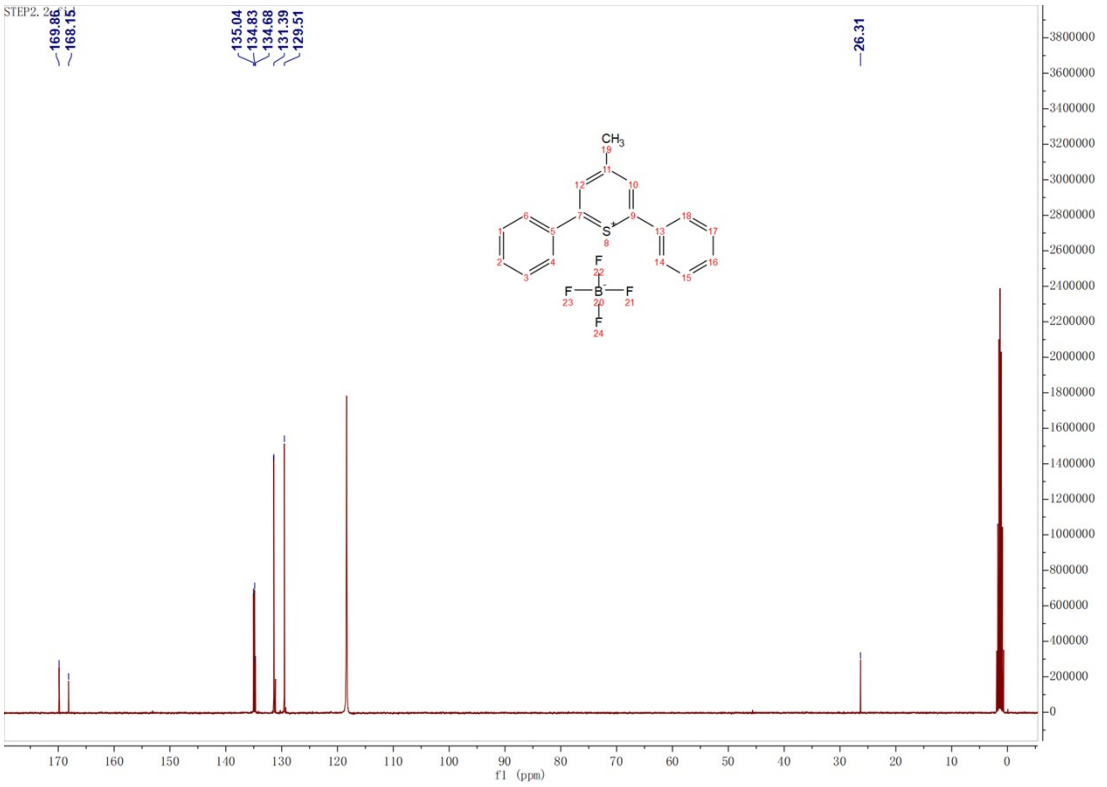

Figure S33. ^{13}C NMR spectrum of **4**.

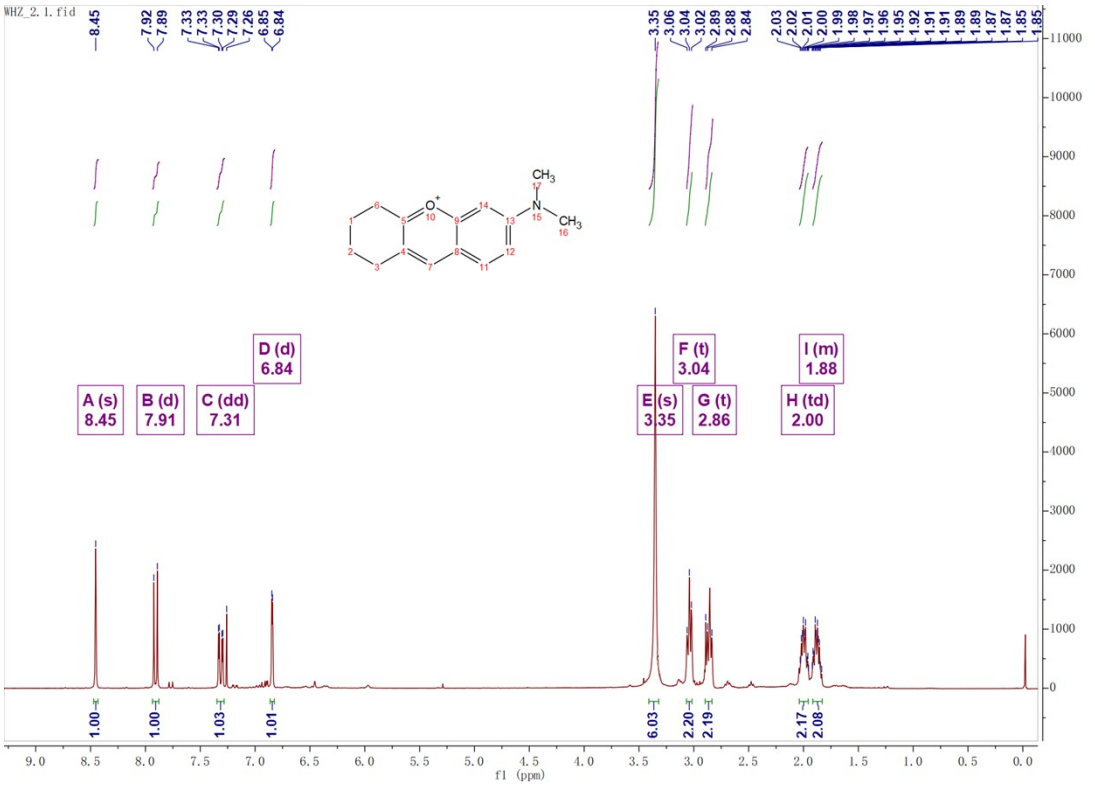

Figure S34. ^{1}H NMR spectrum of **5**.

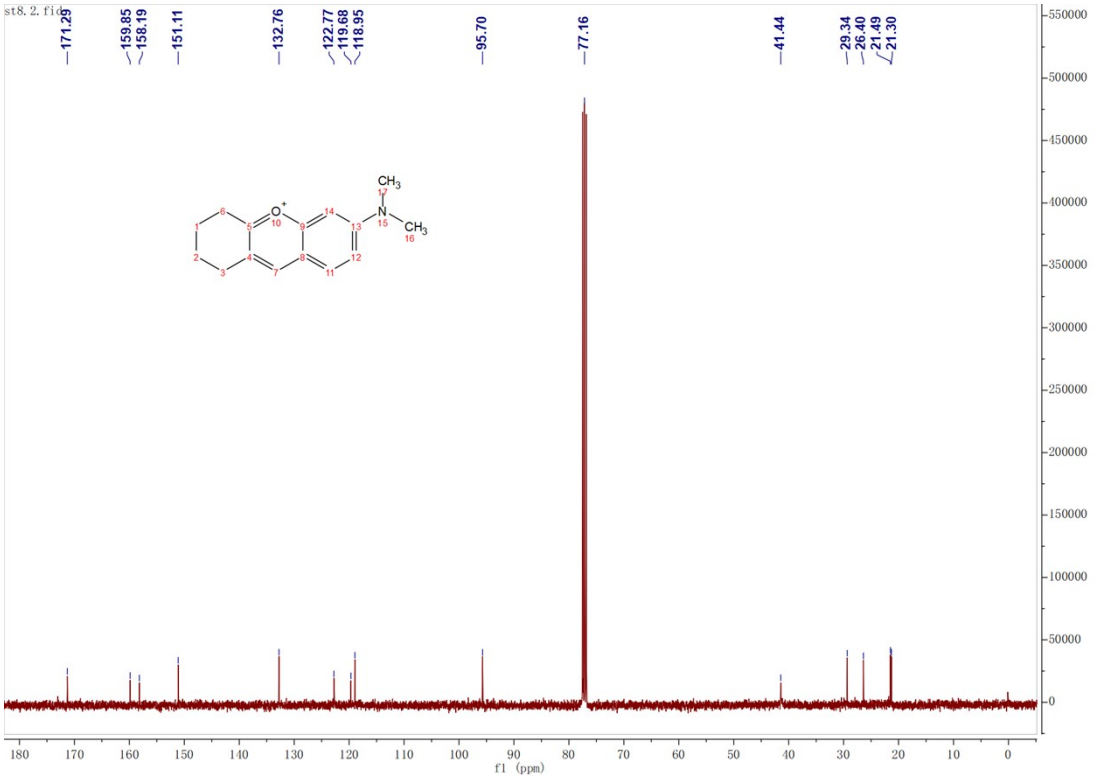

Figure S35. ^{13}C NMR spectrum of **5**.

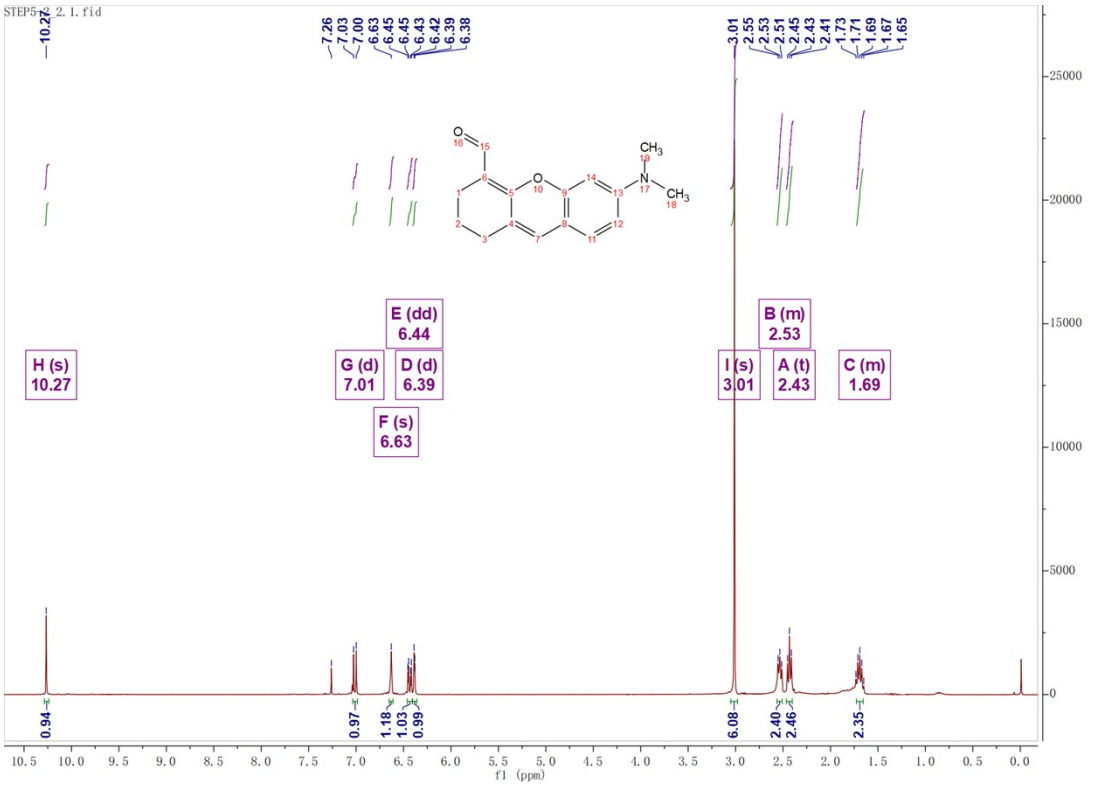

Figure S36.. ^{1}H NMR spectrum of **6**.

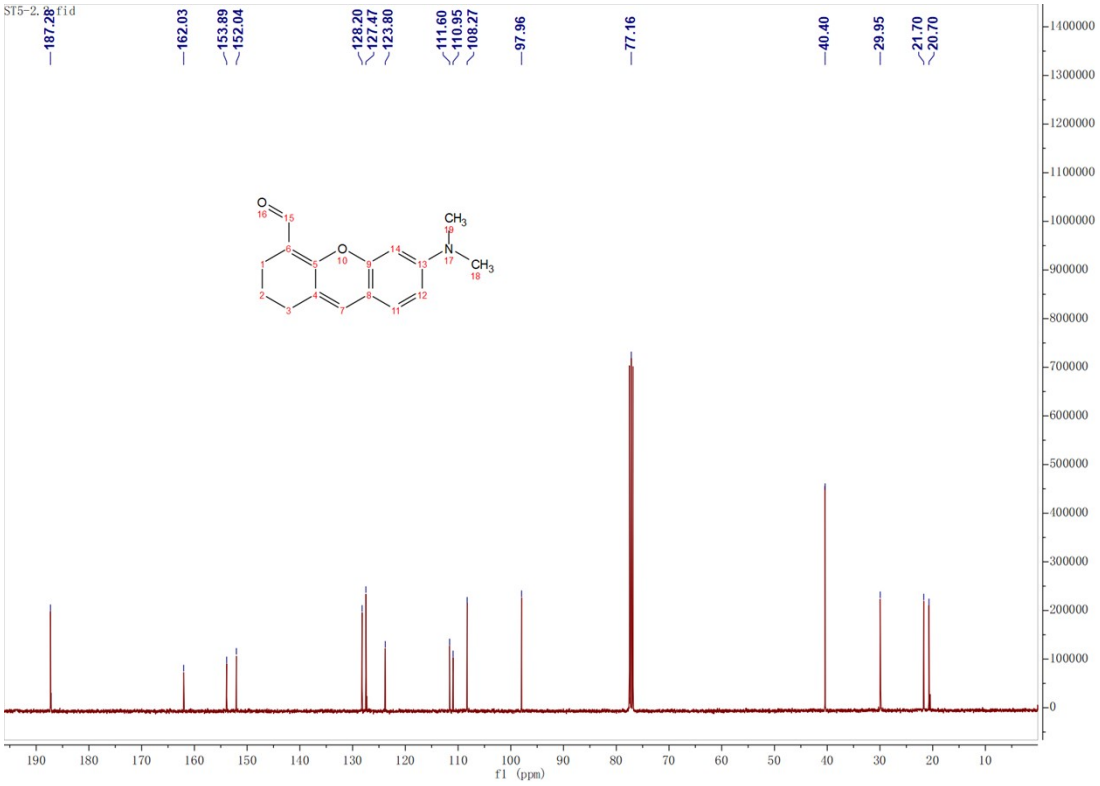

Figure S37. ^{13}C NMR spectrum of **6**.

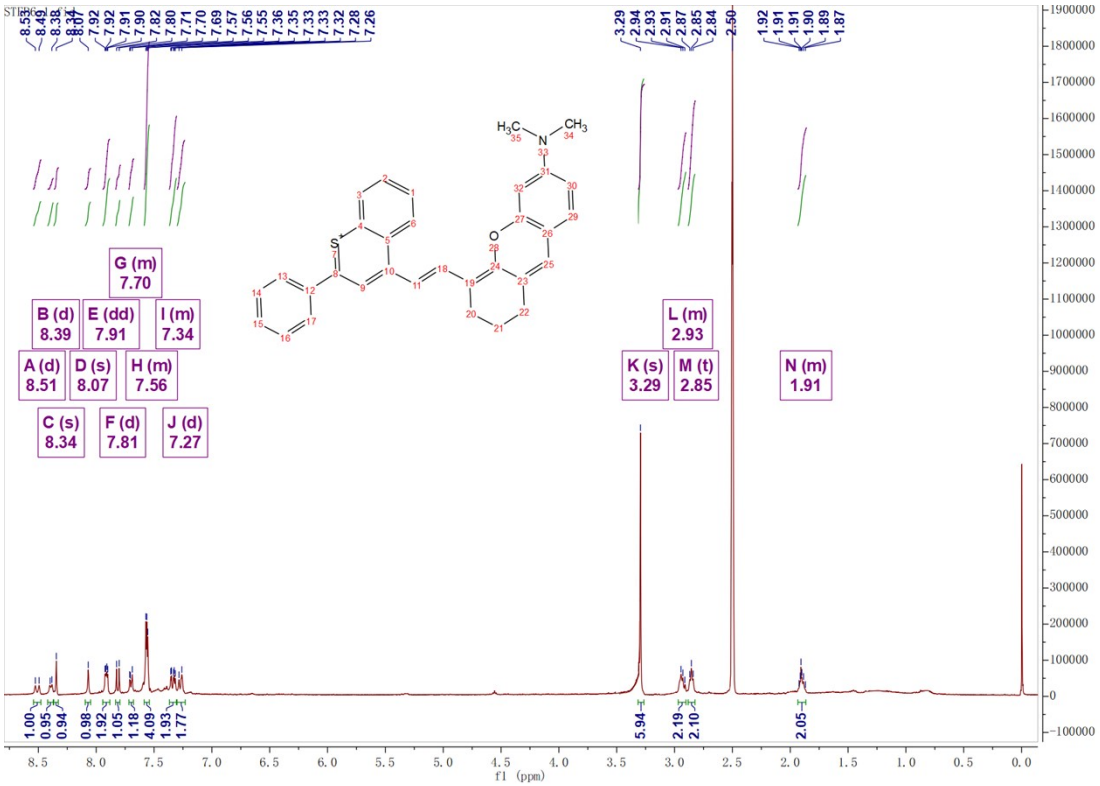

Figure S38. ^{1}H NMR spectrum of **ATX-1**.

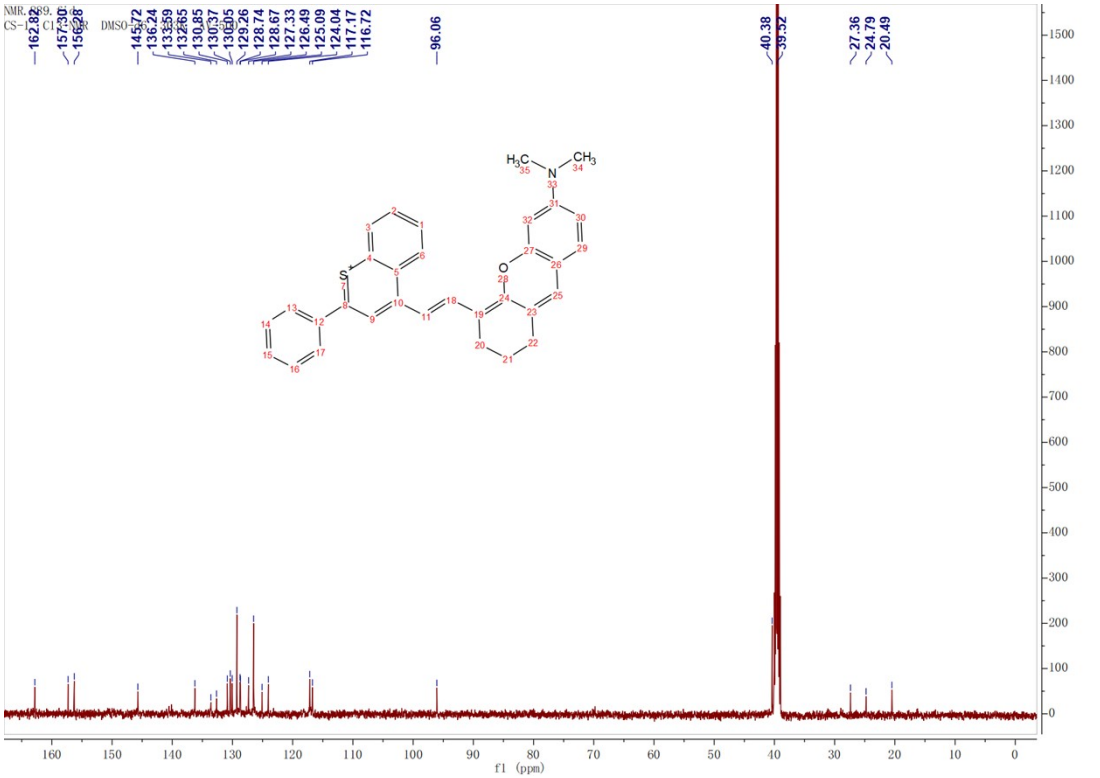

Figure S39. ^{13}C NMR spectrum of **ATX-1**.

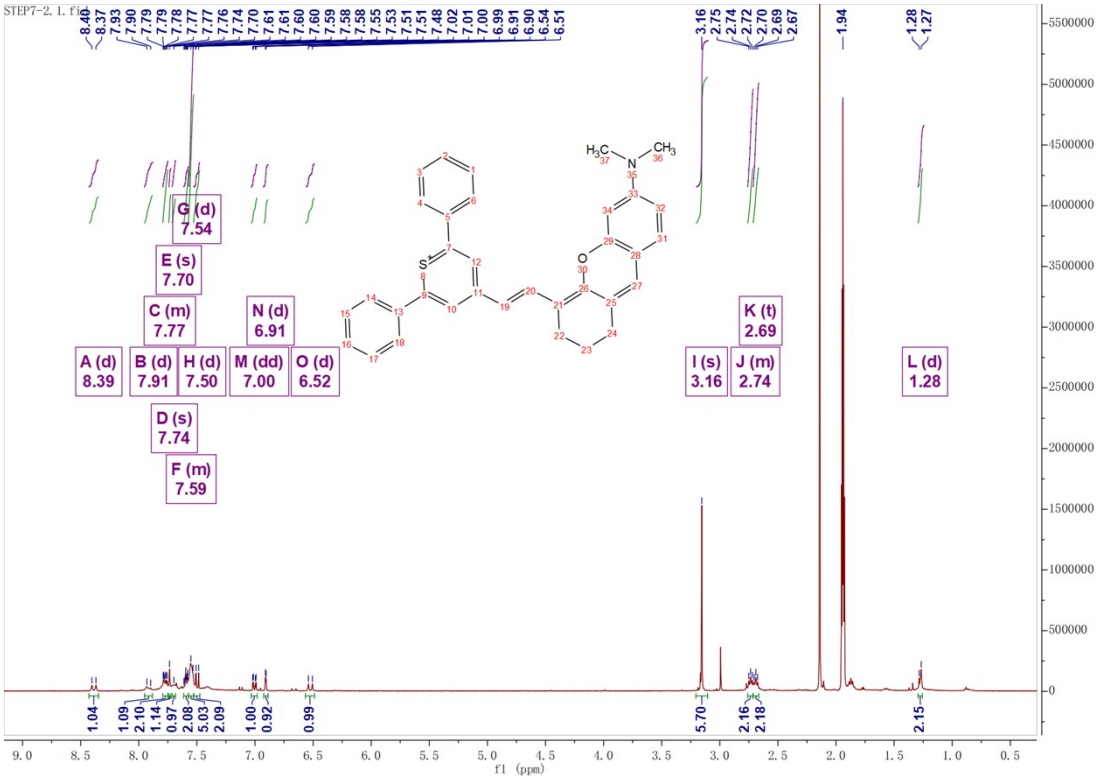

Figure S40. ^{1}H NMR spectrum of **ATX-2**.

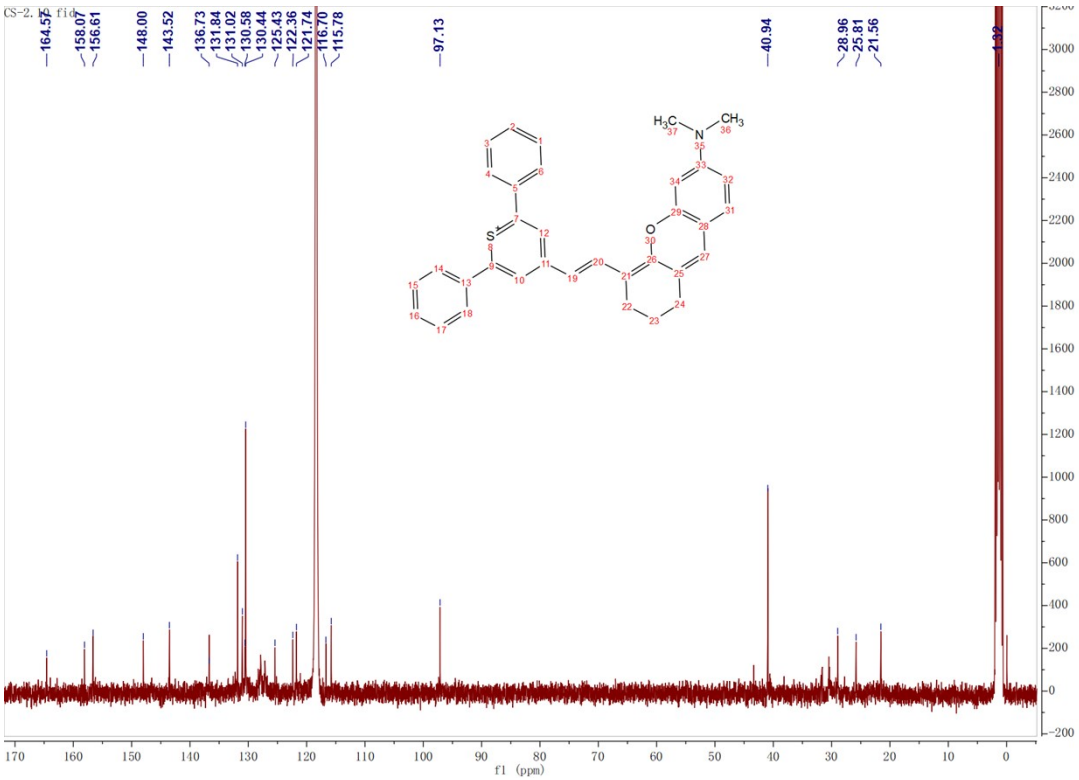

Figure S41. ^{13}C NMR spectrum of **ATX-2**.

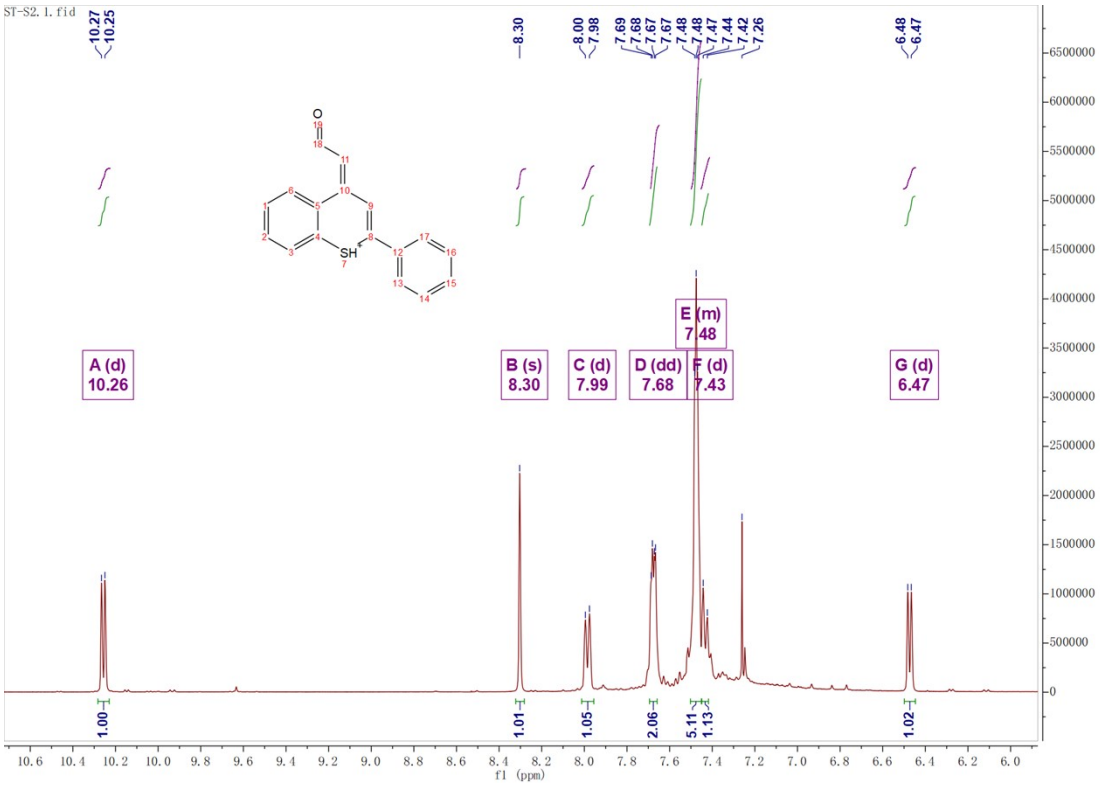

Figure S42. ^{1}H NMR spectrum of **7**.

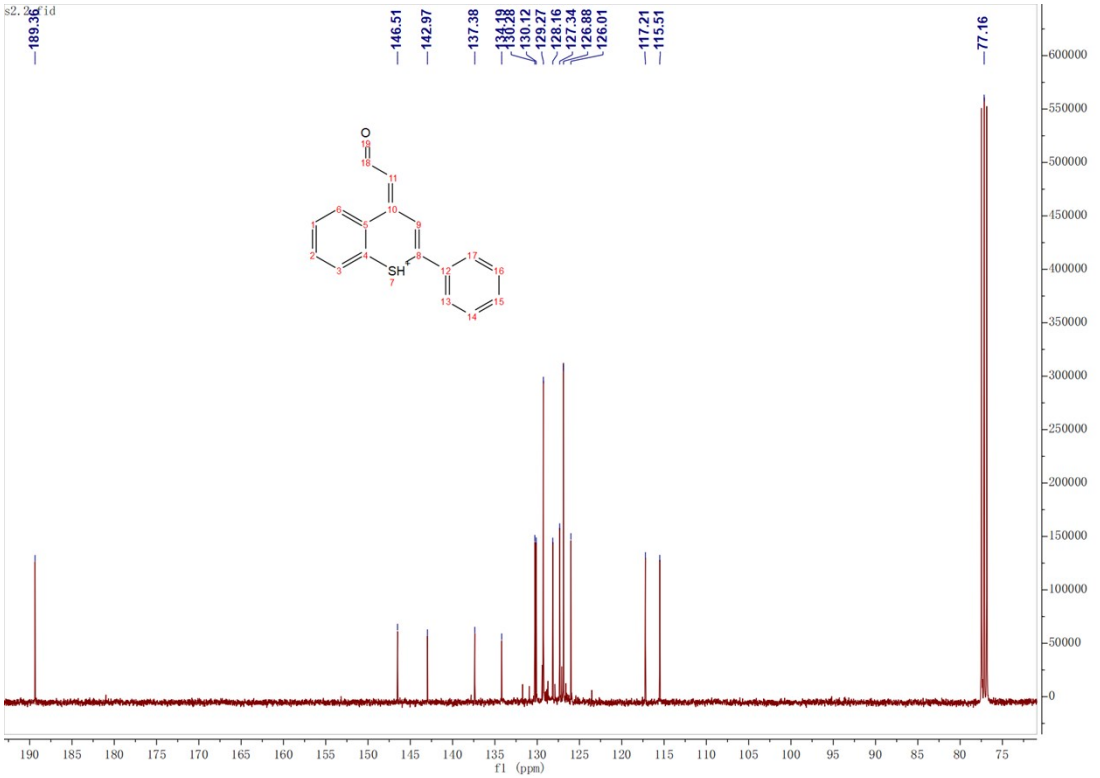

Figure S43. ^{13}C NMR spectrum of **7**.

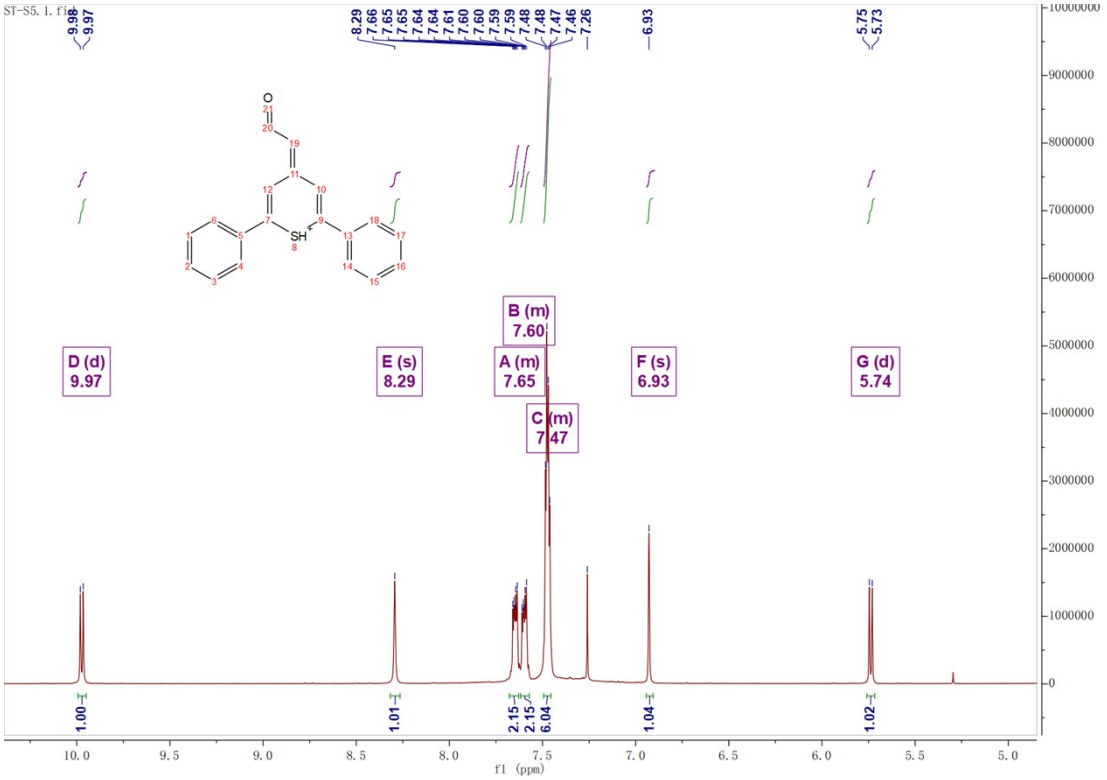

Figure S44. ^{1}H NMR spectrum of **8**.

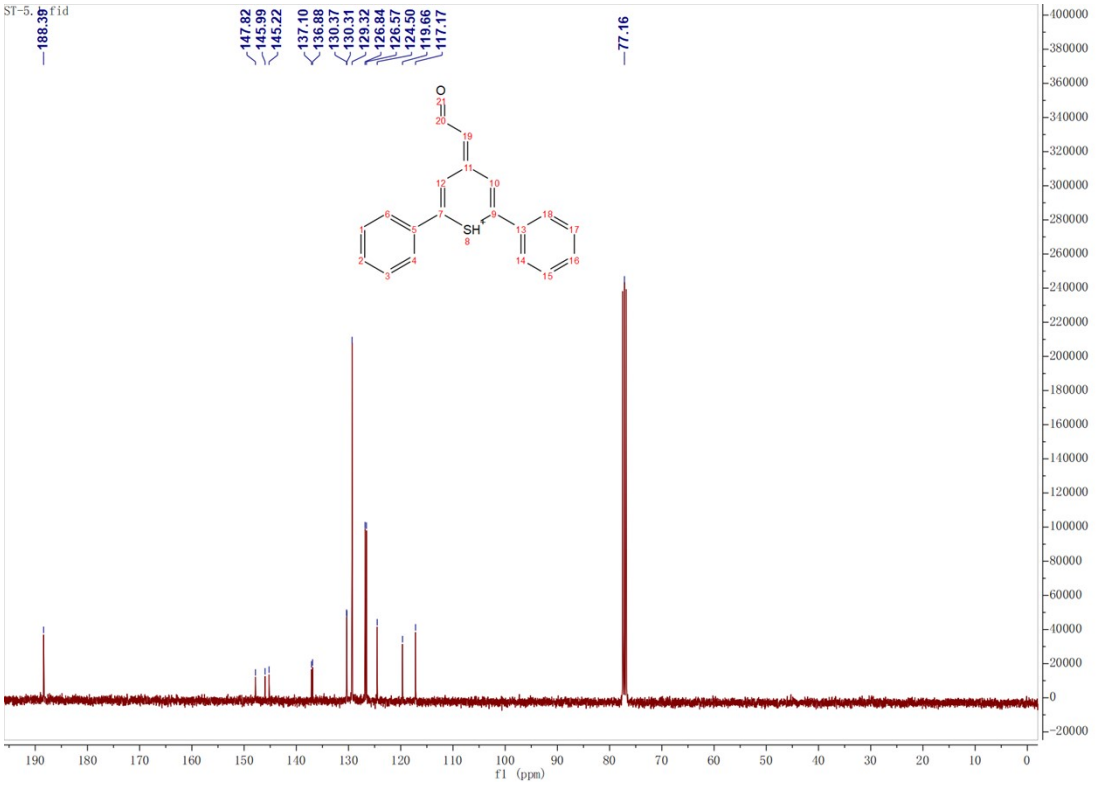

Figure S45. ^{13}C NMR spectrum of **8**.

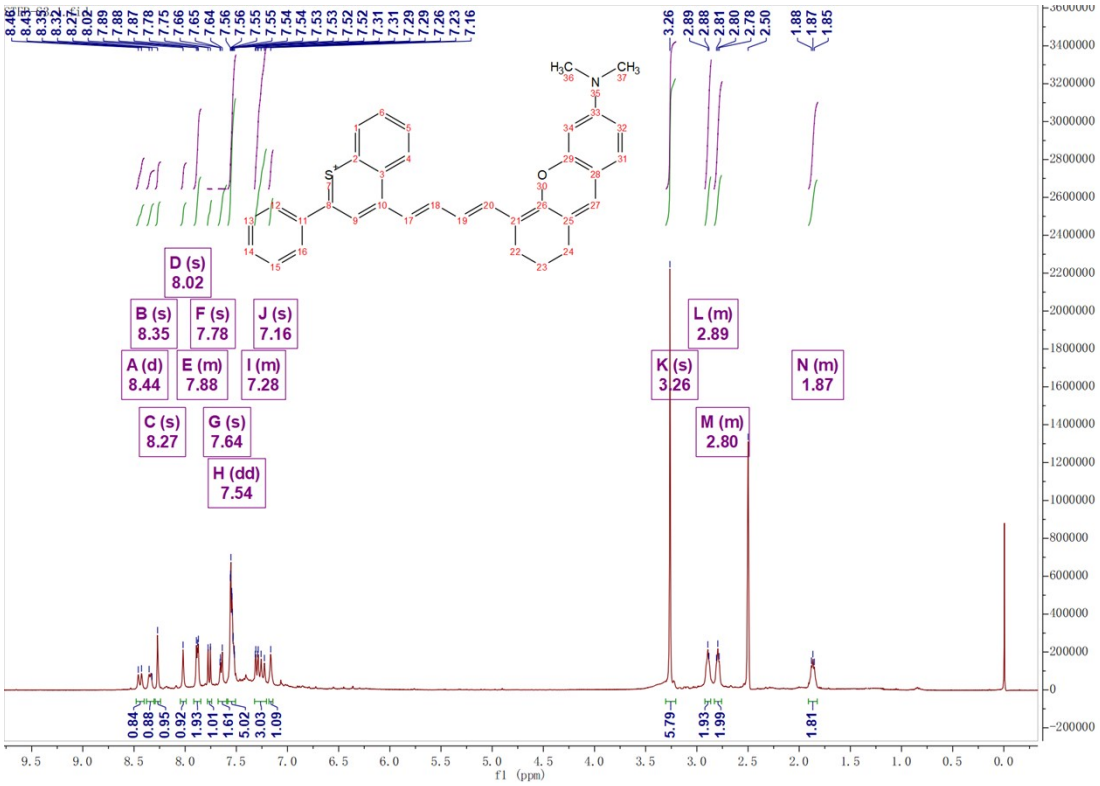

Figure S46. ^{1}H NMR spectrum of **ATX-3**.

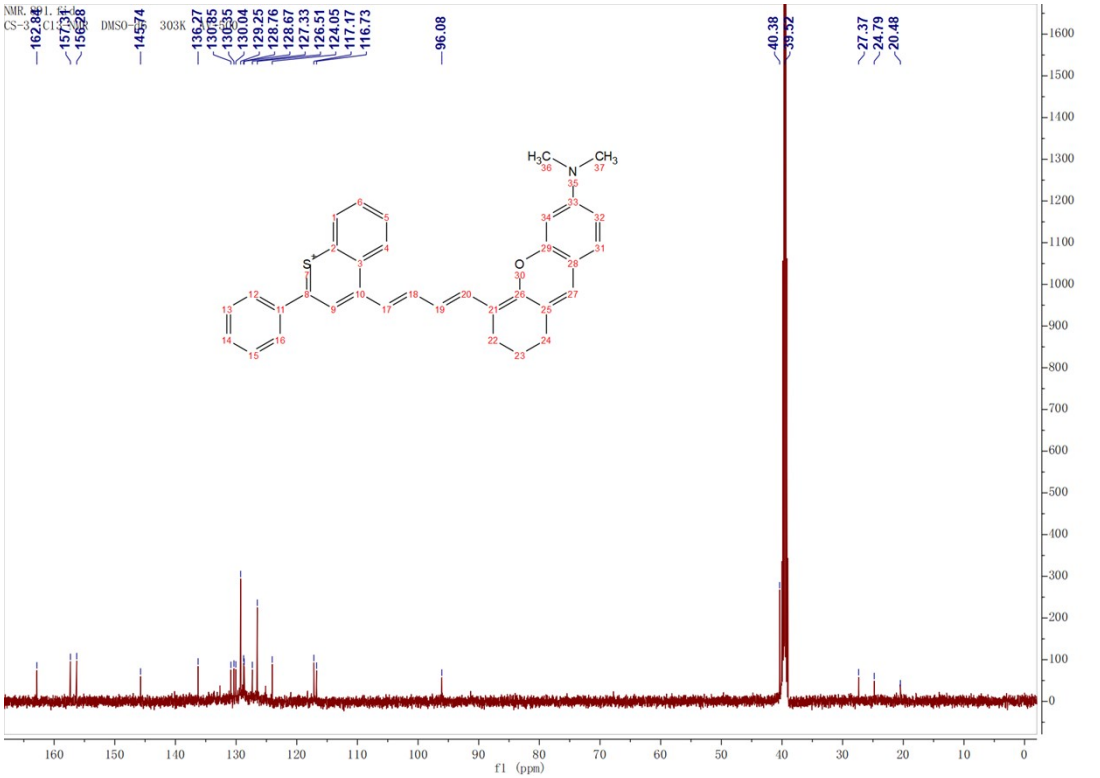

Figure S47. ^{13}C NMR spectrum of **ATX-3**.

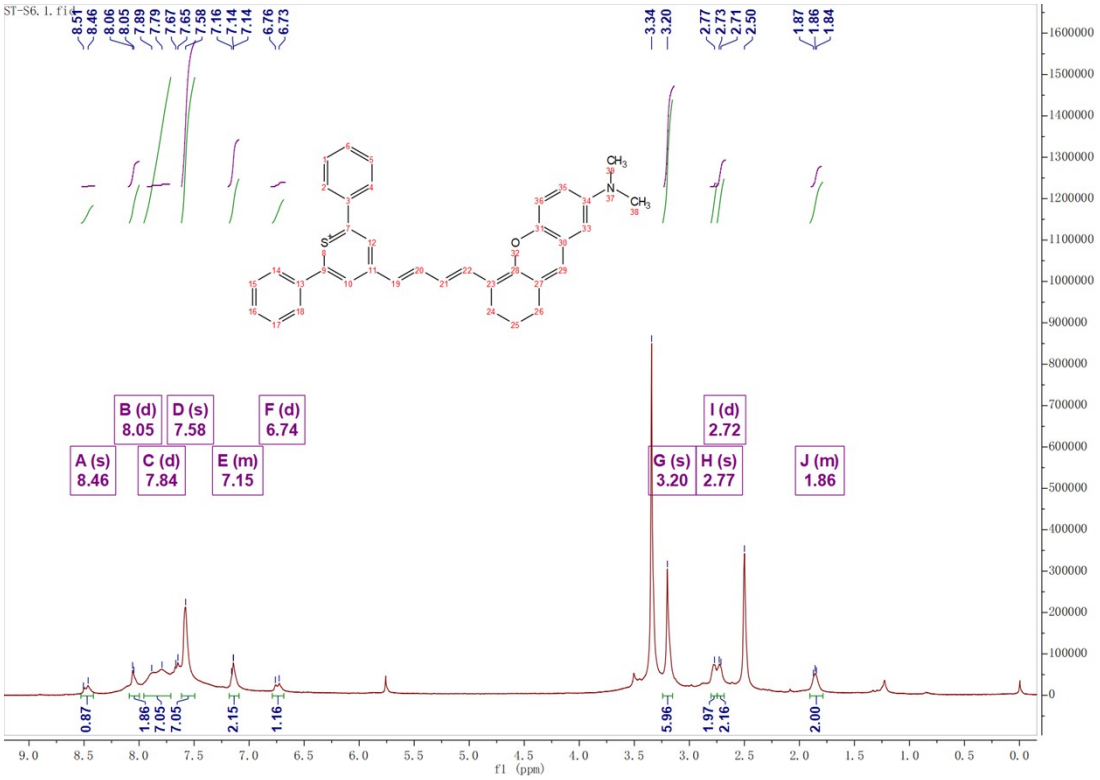

Figure S48. ^{1}H NMR spectrum of **ATX-4**.

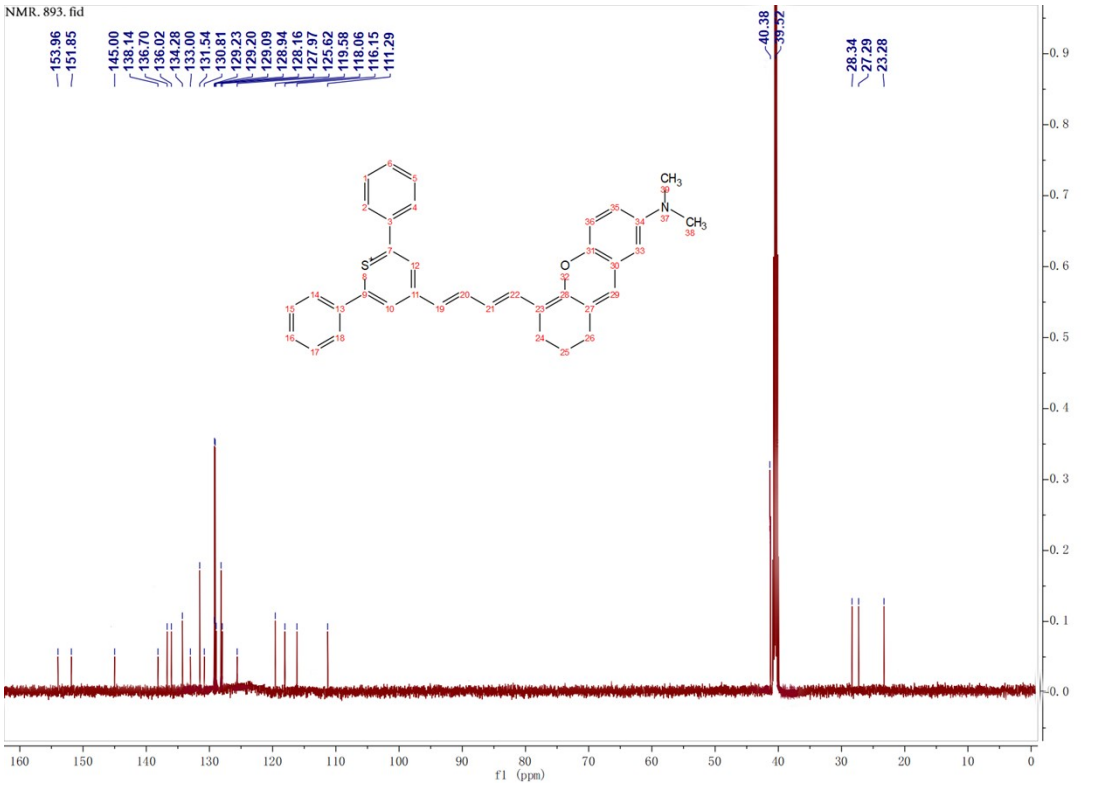

Figure S49. ^{13}C NMR spectrum of **ATX-4**.

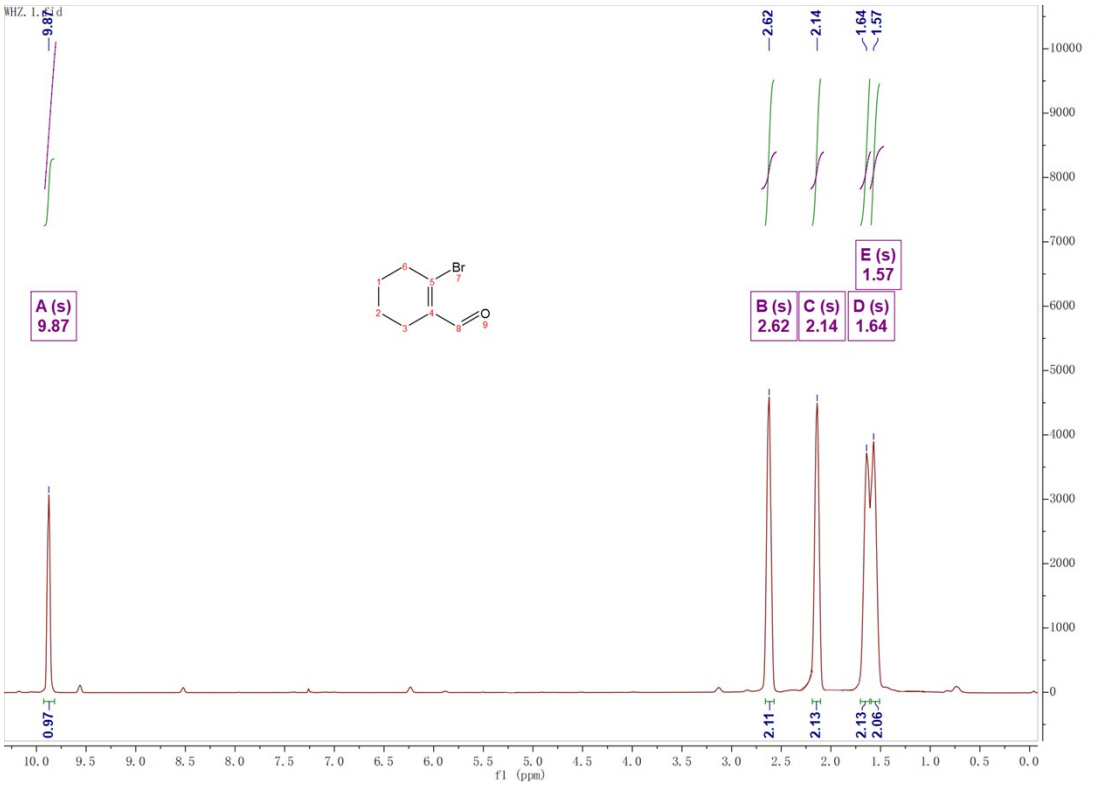

Figure S50. ^{1}H NMR spectrum of **9**.

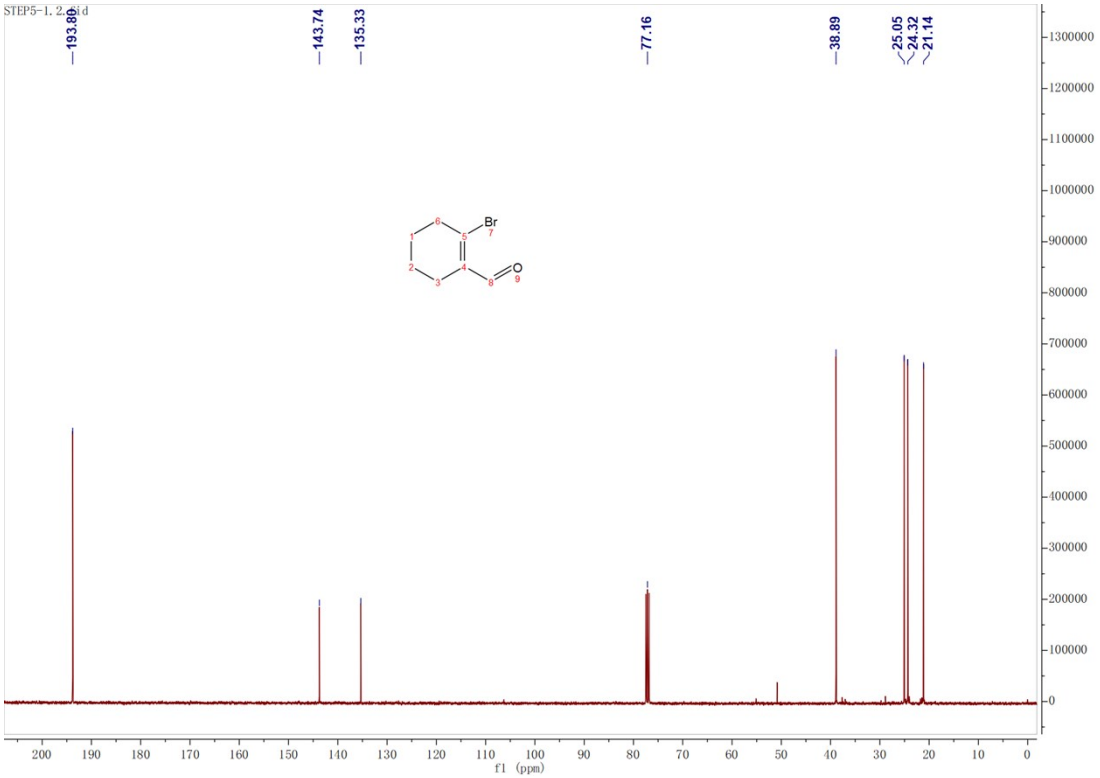

Figure S51. ^{13}C NMR spectrum of **9**.

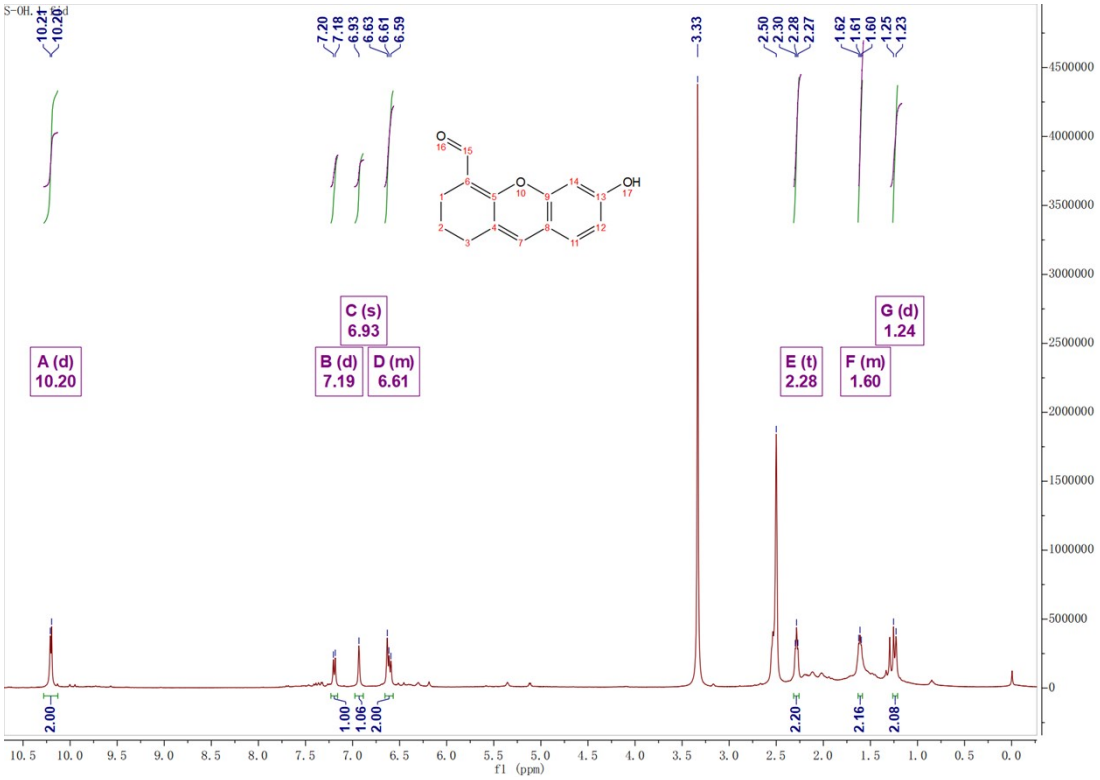

Figure S52. ^{1}H NMR spectrum of **10**.

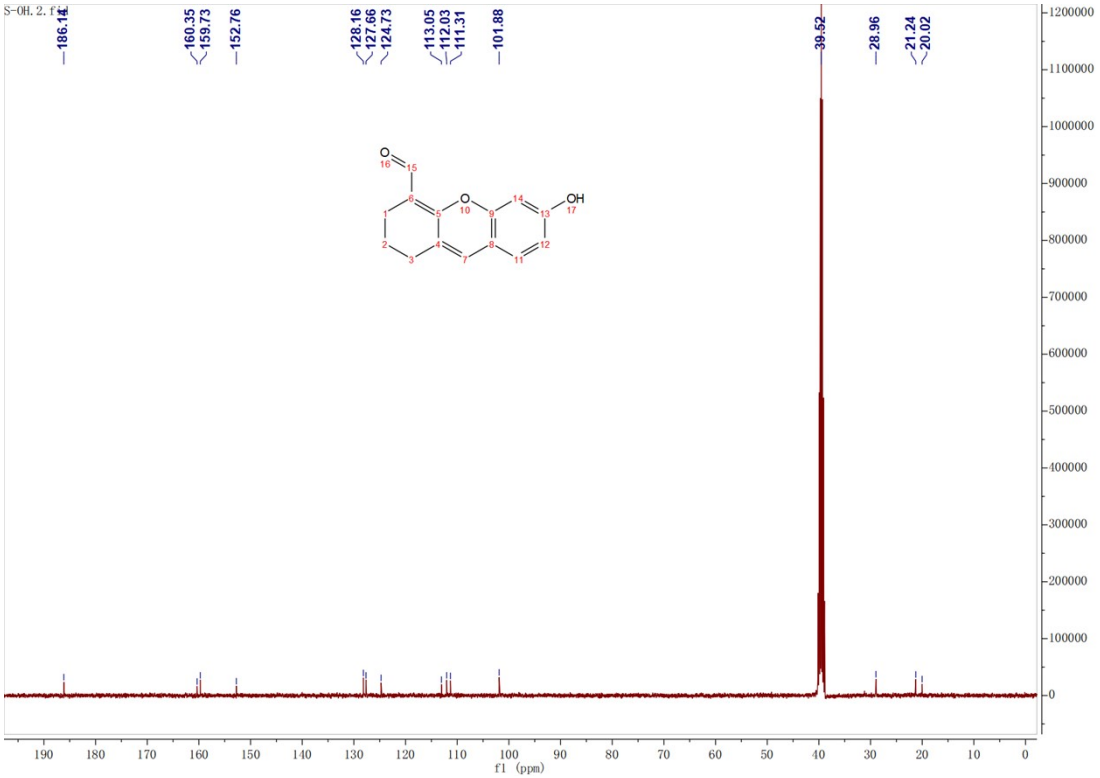

Figure S53. ^{13}C NMR spectrum of **10**.

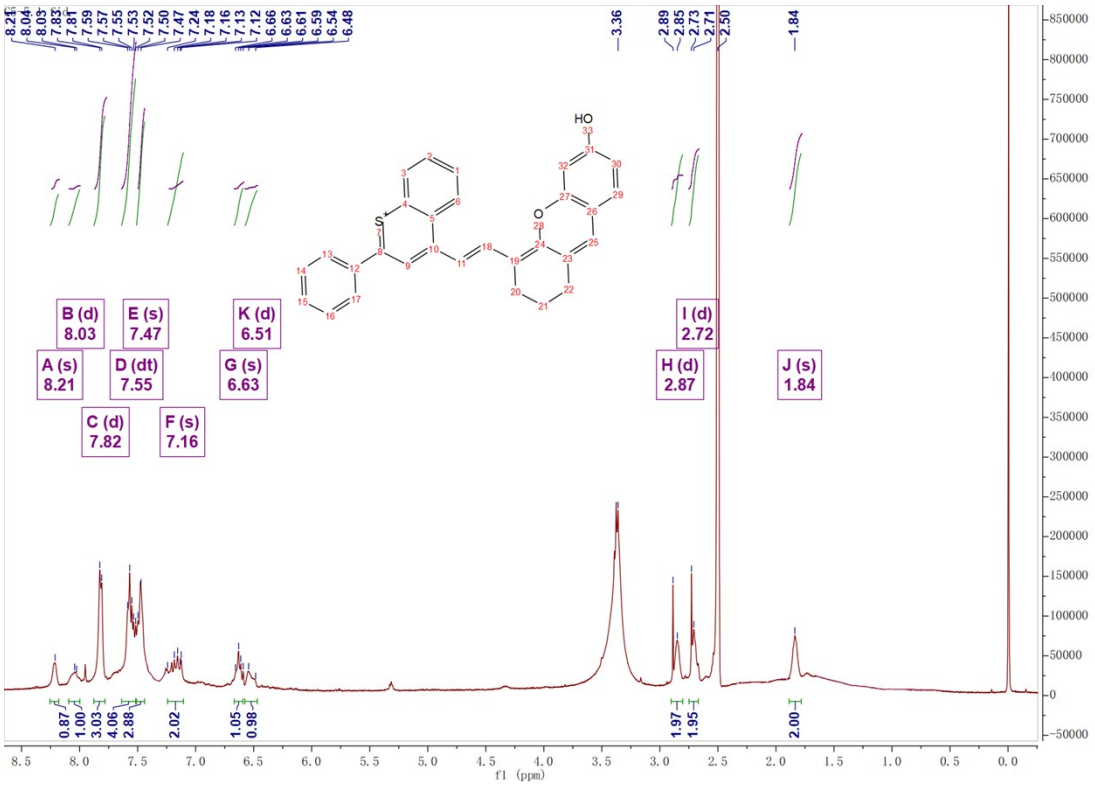

Figure S54. ^{1}H NMR spectrum of **ATX-5**.

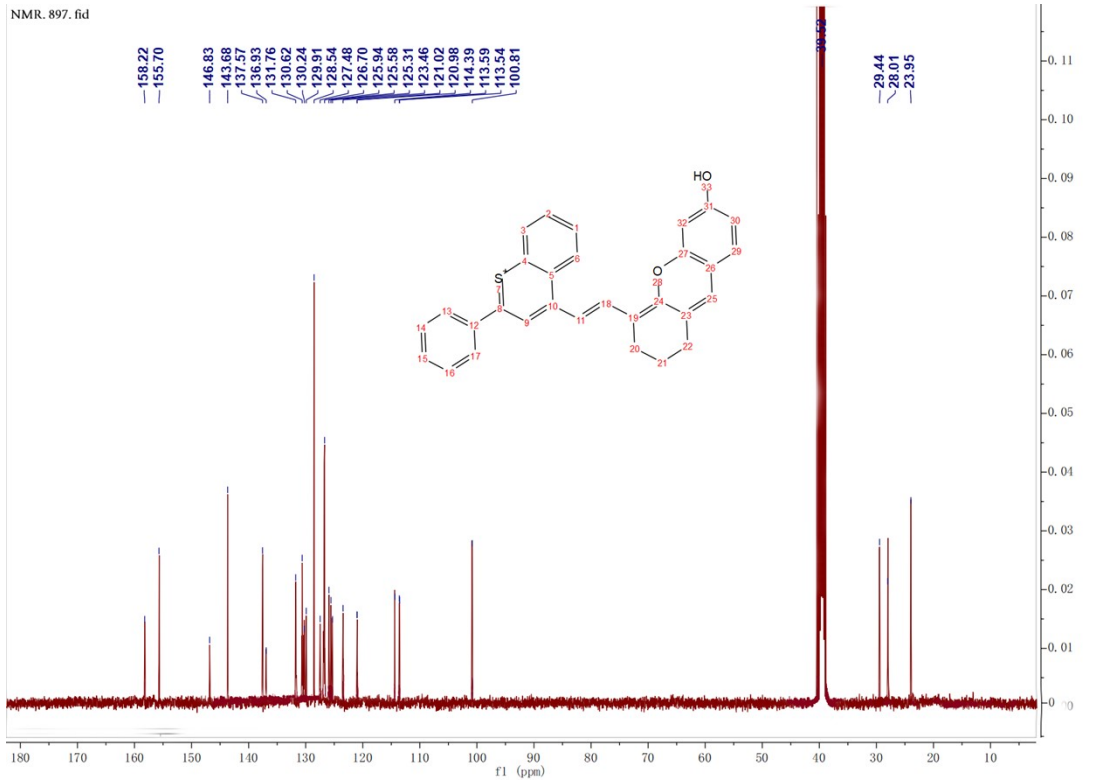

Figure S55. ^{13}C NMR spectrum of **ATX-5**.

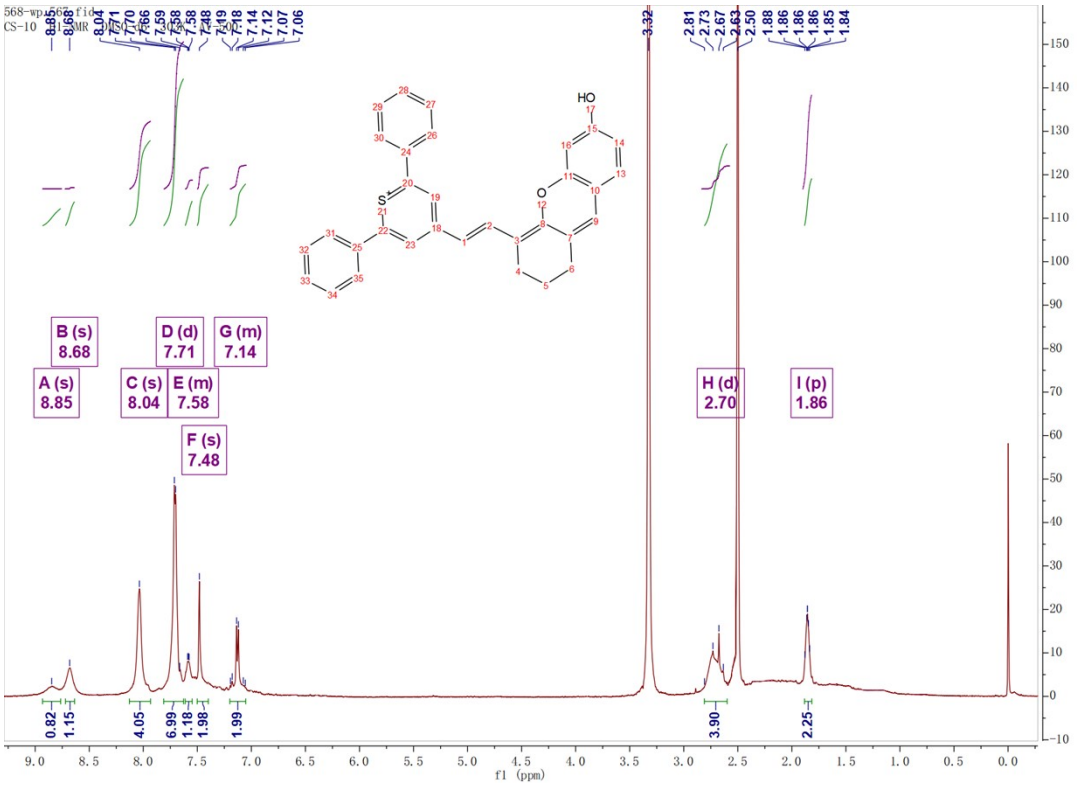

Figure S56. ^{1}H NMR spectrum of **ATX-6**.

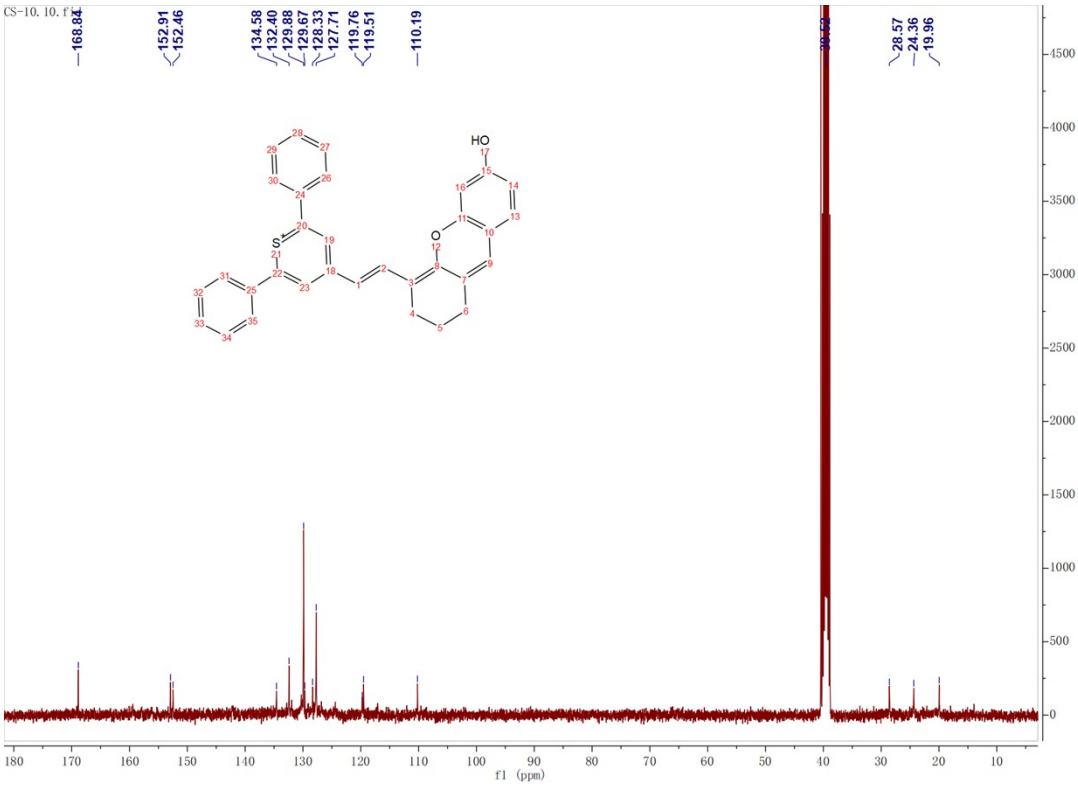

Figure S57. ^{13}C NMR spectrum of **ATX-6**.

Qualitative Analysis Report

Data Filename	20231009-35-1.d	**Sample Name**	CS-1
Sample Type	Sample	**Position**	Vial 35
Instrument Name	Instrument 1	**User Name**	
Acq Method	E+.m	**Acquired Time**	10/9/2023 2:47:39 PM (UTC+08:00)
IRM Calibration Status	Success	**DA Method**	1.m
Comment			

Sample Group		**Info.**	
Stream Name	LC 1	**Acquisition Time (Local)**	10/9/2023 2:47:39 PM (UTC+08:00)
Acquisition SW Version	6200 series TOF/6500 series Q-TOF B.06.01 (B6157)	**TOF Driver Version**	6.00.01
TOF Firmware Version	17.643		

Spectra

Collision Energy 0 **Ionization Mode** ESI

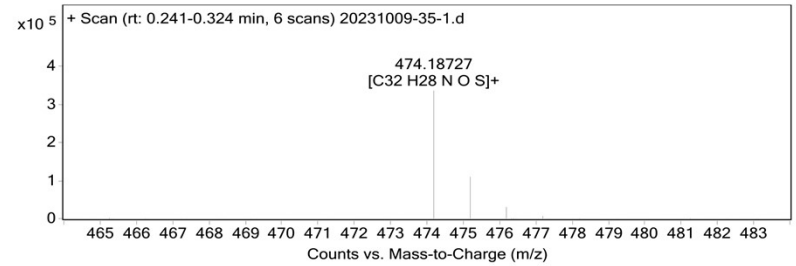

Peak List

m/z	z	Abund	Formula	Ion
64.01663		116097.96		
90.09175	1	131647.45		
111.04186	1	117097.45		
121.05087	1	130639.46		
474.18727	1	335861.84	C32 H28 N O S	M+

Formula Calculator Element Limits

Element	Min	Max
C	30	40
H	25	35
N	1	1
O	1	1
S	1	1

Formula Calculator Results

Formula	Best	Mass	Tgt Mass	Diff (ppm)	Ion Species	CalculatedMz
C32 H28 N O S	TRUE	474.18807	474.18916	2.3	C32 H28 N O S	474.18861

--- End Of Report ---

Figure S58. HRMS of **ATX-1**.

Qualitative Analysis Report

Data Filename	20231009-36-1.d	**Sample Name**	CS-2
Sample Type	Sample	**Position**	Vial 36
Instrument Name	Instrument 1	**User Name**	
Acq Method	E+.m	**Acquired Time**	10/9/2023 2:51:20 PM (UTC+08:00)
IRM Calibration Status	Success	**DA Method**	1.m
Comment			

Sample Group		**Info.**	
Stream Name	LC 1	**Acquisition Time (Local)**	10/9/2023 2:51:20 PM (UTC+08:00)
Acquisition SW Version	6200 series TOF/6500 series Q-TOF B.06.01 (B6157)	**TOF Driver Version**	6.00.01
TOF Firmware Version	17.643		

Spectra

Collision Energy 0 **Ionization Mode** ESI

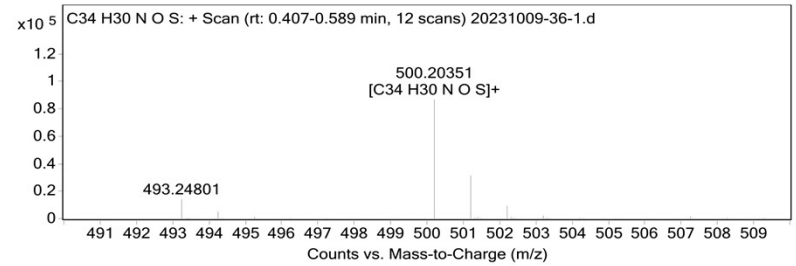

Peak List

m/z	z	Abund
64.01666	1	110307.15
90.09176	1	134805.39
111.04189	1	110455.76
121.05087	1	134656.73
474.18754	1	216427.83

Formula Calculator Element Limits

Element	Min	Max
C	30	40
H	25	35
N	1	1
O	1	1
S	1	1

Formula Calculator Results

Formula	Best	Mass	Tgt Mass	Diff (ppm)	Ion Species	CalculatedMz
C34 H30 N O S	TRUE	500.2042	500.20481	1.21	C34 H30 N O S	500.20426

--- End Of Report ---

Figure S59. HRMS of **ATX-2**.

Qualitative Analysis Report

Data Filename	20231009-37-1.d	**Sample Name**	CS-3
Sample Type	Sample	**Position**	Vial 37
Instrument Name	Instrument 1	**User Name**	
Acq Method	E+.m	**Acquired Time**	10/9/2023 2:55:01 PM (UTC+08:00)
IRM Calibration Status	Success	**DA Method**	1.m
Comment			

Sample Group		**Info.**	
Stream Name	LC 1	**Acquisition Time (Local)**	10/9/2023 2:55:01 PM (UTC+08:00)
Acquisition SW Version	6200 series TOF/6500 series Q-TOF B.06.01 (B6157)	**TOF Driver Version**	6.00.01
TOF Firmware Version	17.643		

Spectra

Collision Energy 0 **Ionization Mode** ESI

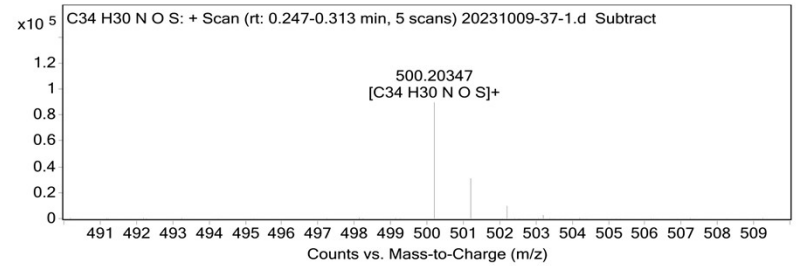

Peak List

m/z	z	Abund	Formula	Ion
474.18759	1	88503.88		
475.19135	1	26765.66		
500.20347	1	89706.49	C34 H30 N O S	M+
501.207	1	31125.13	C34 H30 N O S	M+
736.23366	1	22095.96		

Formula Calculator Element Limits

Element	Min	Max
C	30	40
H	25	35
N	1	1
O	1	1
S	1	1

Formula Calculator Results

Formula	Best	Mass	Tgt Mass	Diff (ppm)	Ion Species	CalculatedMz
C34 H30 N O S	TRUE	500.20409	500.20481	1.45	C34 H30 N O S	500.20426

--- End Of Report ---

Figure S60. HRMS of **ATX-3**.

Qualitative Analysis Report

Data Filename	CS-4.d	**Sample Name**	CS-4
Sample Type	Sample	**Position**	Vial 17
Instrument Name	Instrument 1	**User Name**	
Acq Method	E+R.m	**Acquired Time**	3/20/2024 7:56:52 PM (UTC+08:00)
IRM Calibration Status	Success	**DA Method**	1.m
Comment			

Sample Group		**Info.**	
Stream Name	LC 1	**Acquisition Time (Local)**	3/20/2024 7:56:52 PM (UTC+08:00)
Acquisition SW Version	6200 series TOF/6500 series Q-TOF B.06.01 (B6157)	**TOF Driver Version**	6.00.01
TOF Firmware Version	17.643		

Spectra

Collision Energy 0 **Ionization Mode** ESI

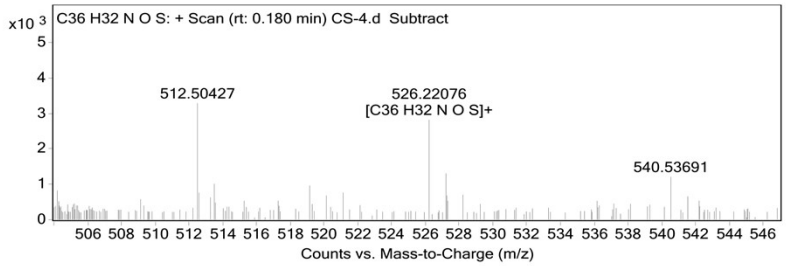

Peak List

m/z	z	Abund
102.12766	1	33567.54
228.13863	1	63728.69
260.16513	1	37300.77
500.20375	1	303369.03
501.2079	1	102929.01

Formula Calculator Element Limits

Element	Min	Max
C	36	36
H	32	32
O	0	3
N	0	1
Br	0	1
S	0	1

Formula Calculator Results

Formula	Best	Mass	Tgt Mass	Diff (ppm)	Ion Species	CalculatedMz
C36 H32 N O S	TRUE	526.22045	526.22046	0.01	C36 H32 N O S	526.21991

--- End Of Report ---

Agilent Technologies Page 1 of 1 Printed at: 8:11 PM on: 3/20/2024

Figure S61. HRMS of **ATX-4**.

Qualitative Analysis Report

Data Filename	CS-5.d	**Sample Name**	CS-5
Sample Type	Sample	**Position**	Vial 29
Instrument Name	Instrument 1	**User Name**	
Acq Method	E+.m	**Acquired Time**	9/19/2023 7:14:32 PM (UTC+08:00)
IRM Calibration Status	Success	**DA Method**	1.m
Comment			

Sample Group		**Info.**	
Stream Name	LC 1	**Acquisition Time (Local)**	9/19/2023 7:14:32 PM (UTC+08:00)
Acquisition SW Version	6200 series TOF/6500 series Q-TOF B.06.01 (B6157)	**TOF Driver Version**	6.00.01
TOF Firmware Version	17.643		

Spectra

Collision Energy 0 **Ionization Mode** ESI

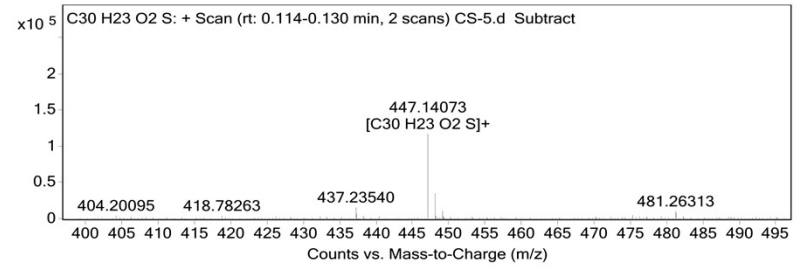

Peak List

m/z	z	Abund	Formula	Ion
64.01663		53366.63		
111.04207		47102.72		
292.11475	1	332008.91		
293.11852	1	63930.61		
447.14073	1	116934.33	C30 H23 O2 S	M+

Formula Calculator Element Limits

Element	Min	Max
C	30	32
H	23	25
O	2	5
S	0	2

Formula Calculator Results

Formula	Best	Mass	Tgt Mass	Diff (ppm)	Ion Species	CalculatedMz
C30 H23 O2 S	TRUE	447.1415	447.14188	0.85	C30 H23 O2 S	447.14133

--- End Of Report ---

Figure S62. HRMS of **ATX-5**.

Qualitative Analysis Report

Data Filename	CS-6.d	**Sample Name**	CS-6
Sample Type	Sample	**Position**	Vial 56
Instrument Name	Instrument 1	**User Name**	
Acq Method	E+R.m	**Acquired Time**	3/14/2024 4:10:45 PM (UTC+08:00)
IRM Calibration Status	Success	**DA Method**	1.m
Comment			

Sample Group		**Info.**	
Stream Name	LC 1	**Acquisition Time (Local)**	3/14/2024 4:10:45 PM (UTC+08:00)
Acquisition SW Version	6200 series TOF/6500 series Q-TOF B.06.01 (B6157)	**TOF Driver Version**	6.00.01
TOF Firmware Version	17.643		

Spectra

Collision Energy 0 **Ionization Mode** ESI

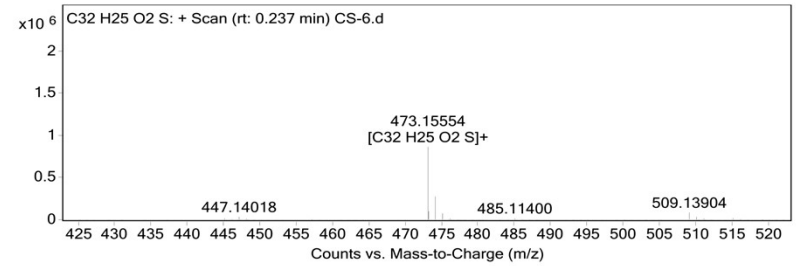

Peak List

m/z	z	Abund	Formula	Ion
90.09138		186419.31		
473.15554	1	861614.25	C32 H25 O2 S	M+
473.22335		99145.88		
474.15933	1	274930.44	C32 H25 O2 S	M+
922.00982	1	97995.84		

Formula Calculator Element Limits

Element	Min	Max
C	32	32
H	25	25
O	0	2
N	0	2
S	0	1

Formula Calculator Results

Formula	Best	Mass	Tgt Mass	Diff (ppm)	Ion Species	CalculatedMz
C32 H25 O2 S	TRUE	473.1564	473.1575	2.45	C32 H25 O2 S	473.15698

--- End Of Report ---

Figure S63. HRMS of **ATX-6**.

Reference:

[1] Y. Liu, Q. Su, M. Chen, Y. Dong, Y. Shi, W. Feng, Z.Y. Wu, and F. Li, Adv. Mater. **2016**, 28: 6625-6630.

[2] J. Ge, M. Lan, B. Zhou, W. Liu, L. Guo, H. Wang, Q. Jia, G. Niu, X. Huang, H. Zhou, X. Meng, P. Wang, C. S. Lee, W. Zhang and X. Han, Nat. Commun. **2014**, 5, 4596.

[3] E. D. Cosco, J. R. Caram, O. T. Bruns, D. Franke, R. A. Day, E. P. Farr, M. G. Bawendi, E. M. Sletten, *Angew. Chem. Int. Ed.* **2017**, *56*, 13126.

[4] P. H. Xiao, W. Xie, J. Zhang, Q. Wu, Z. Shen, C. Guo, Y. Wu, F. Wang, B. Z. Tang, and D. Wang, *J. Am. Chem. Soc*. **2023**, *145*, 334-344.

[5] W. Cao, Y. Zhu, F. Wu, Y. Tian, Z. Chen, W. Xu, S. Liu, T. Liu, H. Xiong, *Small* **2022**, *18*, 2204851.